

Best DBMR Publication Prize 2021

Applicant's declaration

Name: Dr. Tim Rollenske

Address: Murtenstr. 35

E-mail: tim.rollenske@dbmr.unibe.ch

- X I have a DBMR affiliation
- X I have obtained the permission of the co-author(s) of the work submitted, at least one of whom is affiliated with the DBMR.
- X I confirm that the article has a publication date of the year 2021
- X I have attached a short description of my publication stating why my publication is special and should win the prize
- X I have attached the article.

Date: 11.04.2022

Signature:

Tim Rollenske

~~~~~

**Send all documents in one single pdf to: [awards.dbmr@unibe.ch](mailto:awards.dbmr@unibe.ch)**

## Publication Summary

The protective effect of antibodies in infection is well-studied. However, in non-pathogenic host-microbe interactions, such as the intestinal exposure to microbiota, the role of antibodies is less clear. In the publication “**Parallelism of intestinal secretory IgA shapes functional microbial fitness**” published in *Nature* in 2021 we show how luminal secretory IgA antibodies exert control on our intestinal bacteria. By using single B cell Ig gene sequencing, newly established monoclonal dimeric recombinant mouse IgA antibody production and numerous antibody-antigen binding assays we describe the properties of a panel of antigen-specific monoclonal IgA species derived from single intestinal plasma cells. Using antibody supplementation in mono-colonized antibody-deficient animals, we studied the impact of intestinal IgA on host-microbial mutualism at monoclonal level. This *in vivo* model and several *in vitro* experiments enabled us to define that a single monoclonal IgA species can control our intestinal bacteria by several distinct mechanisms that act at the same time. In other words, the components of the overall intestinal IgA response act on nutrient uptake, bacterial metabolism, phage susceptibility, aggregation, bile acid-induced membrane damage and bacterial motility, in parallel. Our basic findings may pave the way to use antigen-specific monoclonal IgA to manipulate our intestinal microbiota and improve mucosal vaccination.

*Parallelism of intestinal secretory IgA shapes functional microbial fitness.*

Rollenske, T.\*, Burkhalter, S., Muerner, L. *et al.*, *Nature* **598**, 657–661 (2021).

\* first and shared corresponding author

Word count: 230/400

## CV

### 1. Personal information:

Dr. rer. nat. Tim Rollenske  
Mucosal Immunology  
University Clinics for Visceral Surgery  
Department for Biomedical Research  
Inselspital  
University of Bern  
Murtenstr. 35  
3008 Bern  
+41 (0) 78 237 42 24  
tim.rollenske@dbmr.unibe.ch  
ORCID-ID: 0000-0003-1982-3253



### 2. Education:

01/2017 – PhD, title: “Humans naturally acquire cross-specific anti-glycan antibodies”, supervision: Prof. Dr. Hedda Wardemann, German Cancer Research Center

08/2012 – Diploma (MSc equivalent) of “molecular biology”

### 3. Employment history:

|                   |                                                                                                                                                                                                                                        |
|-------------------|----------------------------------------------------------------------------------------------------------------------------------------------------------------------------------------------------------------------------------------|
| 02/2018 – 07/2021 | Postdoctoral fellow<br>Supervision: Prof. Dr. Andrew Macpherson<br>(Inselspital, Bern, Switzerland)                                                                                                                                    |
| 02/2018 – 07/2021 | Postdoctoral fellow<br>Supervision: Prof. Dr. Andrew Macpherson<br>(Maurice Müller Laboratories, Bern, Switzerland)                                                                                                                    |
| 02/2017 – 01/2018 | Postdoctoral fellow,<br>Supervision: Prof. Dr. Hedda Wardemann<br>(German Cancer Research Center, Heidelberg, Germany)                                                                                                                 |
| 09/2012 – 01/2017 | PhD thesis “Humans naturally acquire cross-specific anti-glycan antibodies”<br>Supervision: Prof. Dr. Hedda Wardemann<br>(Max-Planck Institute for Infection Biology, Berlin, Germany<br>since 09/2014: German Cancer Research Center) |

### 4. Institutional responsibilities:

Flow cytometry courses for new group members, support maintenance of the germ-free mouse facility and provide scientific advice on immune repertoire data

### 5. Approved research projects as principal investigator (PI):

|         |                                                                                                                                     |
|---------|-------------------------------------------------------------------------------------------------------------------------------------|
| 12/2021 | Career development grant of the Multidisciplinary center for infectious diseases (University of Bern) (Granted amount: 237.959 CHF) |
|---------|-------------------------------------------------------------------------------------------------------------------------------------|

**7. Teaching:**

|                |                                                                           |
|----------------|---------------------------------------------------------------------------|
| 2014 – present | Direct supervision of 3 undergraduate students and 3 technicians          |
| 2018 - present | lectures and practical courses in the Master of Biomedical Sciences, Bern |

**8. Professional activities:**

|                   |                                                                                                                            |
|-------------------|----------------------------------------------------------------------------------------------------------------------------|
| 02/2013 – 01/2018 | Member of the scientific advisory board for KLEBSICURE Eurostars grant including partners from academia and private sector |
| 06/2013 – 06/2014 | PhD representative of the Max-Planck Institute for Infection Biology                                                       |
| 2020 – present    | Reviewer for eLife                                                                                                         |

**9. Active memberships:**

|                |                                                        |
|----------------|--------------------------------------------------------|
| 2018 – present | German Society of Immunology, Biology of B lymphocytes |
|----------------|--------------------------------------------------------|

**11. Prices, awards and fellowships:**

|         |                                                                                                                   |
|---------|-------------------------------------------------------------------------------------------------------------------|
| 12/2021 | Travel grant at the B cell Keystone meeting                                                                       |
| 10/2020 | PhD prize of the Paul Ehrlich society of chemotherapy                                                             |
| 12/2018 | Granting of an EMBO Long-term postdoctoral fellowship                                                             |
| 05/2015 | Travel grant at the ESF Conference                                                                                |
| 09/2012 | Offer of a PhD stipend from the International Max-Planck Research School for Infectious Diseases and Inflammation |

**Additional information:**

|                   |                                                                                                                                                                      |
|-------------------|----------------------------------------------------------------------------------------------------------------------------------------------------------------------|
| 06/2015 – 05/2018 | Due to pending patent negotiations and patent filing I obtained restrictions by the Max Planck society to publish my results or present at international conferences |
|-------------------|----------------------------------------------------------------------------------------------------------------------------------------------------------------------|

# Parallelism of intestinal secretory IgA shapes functional microbial fitness

<https://doi.org/10.1038/s41586-021-03973-7>

Received: 16 February 2021

Accepted: 31 August 2021

Published online: 13 October 2021

 Check for updates

Tim Rollenske<sup>1✉</sup>, Sophie Burkhalter<sup>1</sup>, Lukas Muerner<sup>2</sup>, Stephan von Gunten<sup>2</sup>, Jolanta Lukasiewicz<sup>3</sup>, Hedda Wardemann<sup>4,5</sup> & Andrew J. Macpherson<sup>1,5✉</sup>

Dimeric IgA secreted across mucous membranes in response to nonpathogenic taxa of the microbiota accounts for most antibody production in mammals. Diverse binding specificities can be detected within the polyclonal mucosal IgA antibody response<sup>1–10</sup>, but limited monoclonal hybridomas have been studied to relate antigen specificity or polyreactive binding to functional effects on microbial physiology in vivo<sup>11–17</sup>. Here we use recombinant dimeric monoclonal IgAs (mIgAs) to finely map the intestinal plasma cell response to microbial colonization with a single microorganism in mice. We identify a range of antigen-specific mIgA molecules targeting defined surface and nonsurface membrane antigens. Secretion of individual dimeric mIgAs targeting different antigens in vivo showed distinct alterations in the function and metabolism of intestinal bacteria, largely through specific binding. Even in cases in which the same microbial antigen is targeted, microbial metabolic alterations differed depending on IgA epitope specificity. By contrast, bacterial surface coating generally reduced motility and limited bile acid toxicity. The overall intestinal IgA response to a single microbe therefore contains parallel components with distinct effects on microbial carbon-source uptake, bacteriophage susceptibility, motility and membrane integrity.

To determine the range of different effects that secretory IgA (SIgA) exerts on microbial metabolism and physiology, we exposed germ-free mice to the auxotrophic commensal model bacteria *Escherichia coli* HA107 (ref. <sup>18</sup>) to induce luminal intestinal *E. coli*-binding SIgA in all animals 21 days later (Extended Data Fig. 1a, b). Almost all single B220<sup>low</sup>IgA<sup>+</sup> lamina propria plasma cells expressed *Igha* transcripts with varying degrees of IgA oligoclonality between mice<sup>11,19</sup> (Extended Data Fig. 1c–e). Each mouse expressed a diverse and unique immunoglobulin gene repertoire with no increase in somatic hypermutation after HA107 exposure (Extended Data Fig. 1f, g).

We expressed a panel of 91 recombinant plasma cell monoclonal antibodies from three different mice (Supplementary Table 1). Recombinant monoclonal IgG-antibodies were screened as human IgG1 to assess antibody binding without avidity effects in polymers (Extended Data Fig. 1h). IgA-expressing plasma cells were not analysed further as they had not increased in frequency after HA107 exposure (Extended Data Fig. 1i). *E. coli* HA107 binding either in flow cytometry against intact HA107 bacteria or enzyme-linked immunosorbent assay (ELISA) against its lysate occurred in 17 of 91 (19%) antibodies after HA107 stimulation, but not in 85 monoclonal antibodies from germ-free mice (Extended Data Fig. 1j–l and Supplementary Tables 1 and 2). All bacteria-reactive monoclonal antibodies originated from non- or low-expanded plasma cells with low or no somatic hypermutations, suggesting recent recruitment into the plasma cell population (Extended Data Fig. 1m, n). Thus, short-term microbial exposure induced diverse low-mutated Ig clones able to coat the inducing bacterium.

After re-expressing the monoclonal antibodies in their original form as dimeric IgA with a IgJ-chain vector (Extended Data Fig. 2a), we reconfirmed binding of 16 mIgAs to intact HA107 or its lysate, with additional antibodies (mIgA<sub>4038</sub>, mIgA<sub>4052</sub> and mIgA<sub>4234</sub>) able to weakly coat the HA107 surface or its JM83 parental strain, presumably due to higher avidity of the dimeric IgA compared to the monomeric IgG form (Fig. 1a, b and Extended Data Fig. 2b, c).

Bacterial surface gene expression varies in vivo and the mammalian intestine also contains damaged bacteria<sup>20</sup>. Using bacterial live/dead discrimination in flow cytometric antibody-binding assays, we detected three different mIgA<sup>+</sup> bacterial populations in faeces of JM83 monoclonalized mice, designated nonreplicating (Syto9<sup>int</sup>propidium iodide (PI)<sup>−</sup>), replicating (Syto9<sup>high</sup>PI<sup>−</sup>) and dying (Syto9<sup>int</sup>PI<sup>+</sup>) (Extended Data Fig. 2d, e). Nonreplicating bacterial binding ex vivo largely reproduced the binding pattern observed in vitro, except for antibody mIgA<sub>4052</sub> (Fig. 1c and Extended Data Fig. 2f). All surface binders, including mIgA<sub>4052</sub>, bound the replicating or dying bacterial fraction (Fig. 1c and Extended Data Fig. 2f). Notably, mIgA<sub>4219</sub> and mIgA<sub>4584</sub> only bound the bacterial lysate in vitro, but could bind replicating or dying bacteria ex vivo, suggesting that their antigens were only accessible in those subpopulations. Overall, we characterized ten dimeric mIgAs that bound the bacterial surface and six that targeted the bacterial lysate. We suggest that priming by a single microbe rapidly and efficiently selects plasma cells secreting IgAs, which may selectively coat the surface of distinct live and dying microbial subpopulations.

<sup>1</sup>Department of Biomedical Research, University Clinic of Visceral Surgery and Medicine, Inselspital, University of Bern, Bern, Switzerland. <sup>2</sup>Institute of Pharmacology, University of Bern, Bern, Switzerland. <sup>3</sup>Laboratory of Microbial Immunochemistry and Vaccines, Ludwik Hirszfeld Institute of Immunology and Experimental Therapy, Wrocław, Poland. <sup>4</sup>B cell Immunology, German Cancer Research Center, Heidelberg, Germany. <sup>5</sup>These authors contributed equally: Hedda Wardemann, Andrew J. Macpherson. ✉e-mail: tim.rollenske@dbmr.unibe.ch; andrew.macpherson@dbmr.unibe.ch

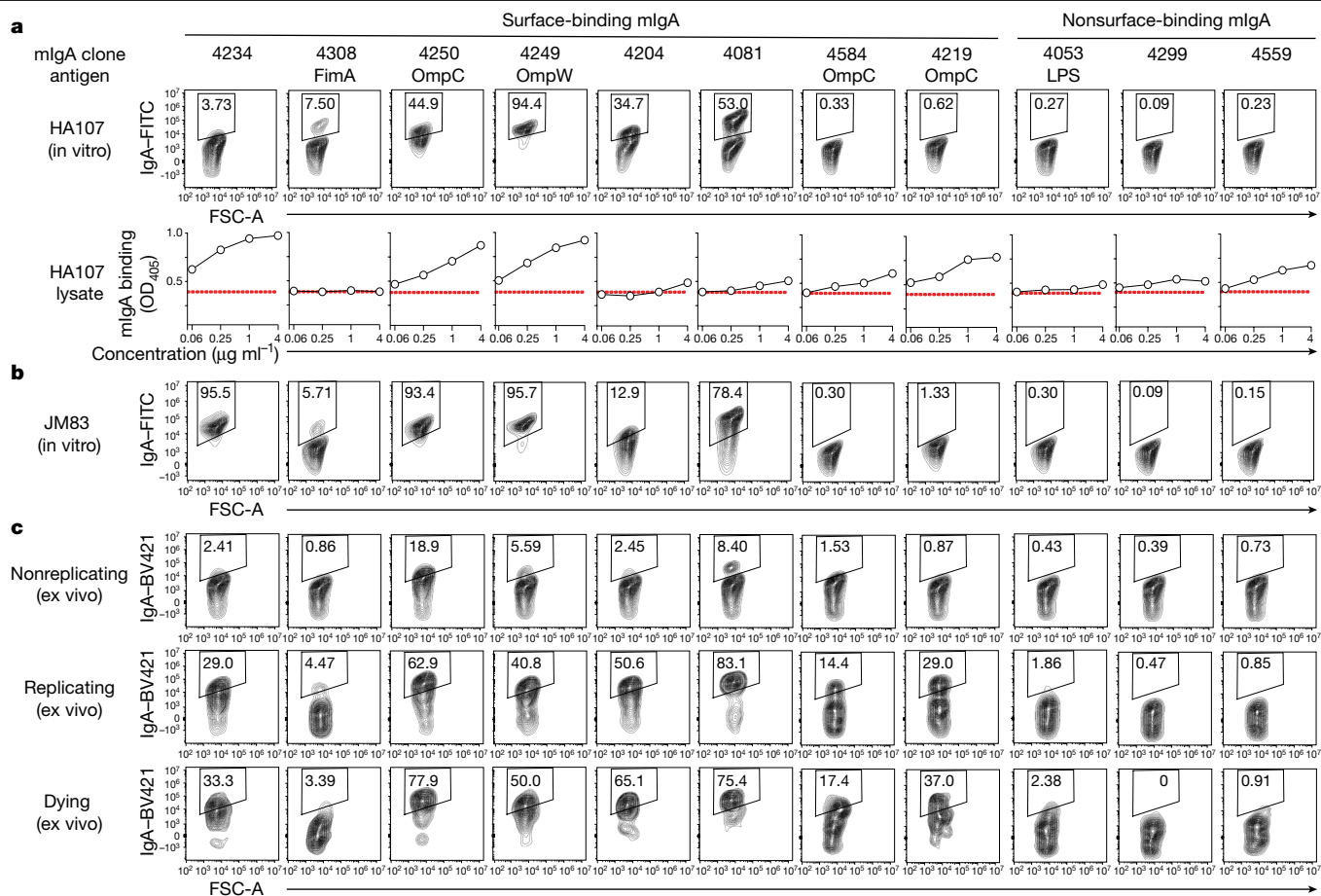


**Fig. 1 | Monoclonal dimeric IgA coats distinct bacterial subpopulations.** **a**, Flow cytometric analysis of individual mlgA binding to intact live HA107 bacteria (top) or HA107 lysate (bottom) by ELISA. Red dashed lines indicate upper binding limit from negative control mlgA<sub>MG053</sub>. **b**, Flow cytometric analysis of

mlgA binding of the non-auxotrophic JM83 parental strain of HA107. **c**, Binding of mlgAs to faecal JM83 nonreplicating (top), replicating (middle) or dying (bottom) subpopulations gated as in Extended Data Fig. 2d. mlgA clones and target antigens are indicated. Data are representative of two independent experiments.

## Dimeric mlgA targets membrane antigens

We confirmed that only the bacterial membrane fraction was targeted by mlgA<sup>21</sup> (Extended Data Fig. 3a, c). This did not require live intact bacteria, as many mlgAs with surface-binding properties, including the two subpopulation binders, also bound outer membrane vesicles (Extended Data Fig. 3b, d).

mlgA<sub>4053</sub> recognized the core region of lipopolysaccharide (LPS) of different rough and smooth *E. coli* LPS structures by ELISA (Extended Data Fig. 4a, b). To identify targeted protein antigens, we screened 782 viable single-deletion *E. coli* mutant strains of the Keio collection for loss of membrane-associated antigen binding in flow cytometry or lysates by ELISA. This identified type I fimbriae as the likely mlgA<sub>4308</sub> target and found that the outer membrane proteins OmpW and OmpC were targeted by mlgA<sub>4249</sub> or mlgA<sub>4250</sub>, mlgA<sub>4219</sub> and mlgA<sub>4584</sub>, respectively (Extended Data Fig. 4c–f and Supplementary Tables 3 and 4).

mlgA<sub>4308</sub>-bound outer membrane vesicle fractions were shown by electron microscopy to contain fimbriae (Extended Data Fig. 4g) as well as the smooth K-12 derivative BW24599, indicating that its antigen exceeds the LPS capsule (Extended Data Fig. 4h). mlgA<sub>4308</sub> binding was not competed by α-methyl-mannoside, supporting Fab-dependent rather than mannose fimbrial lectin attachment (Extended Data Fig. 4i). Separate mlgA<sub>4308</sub>-bound and mlgA<sub>4308</sub>-unbound *E. coli* populations were consistent with fimbrial genetic phase variation, and sorted mlgA<sub>4308</sub>-bound live JM83 populations showed selective expression of type I fimbrial operon genes (Extended Data Fig. 4j). We also directly verified the antigen specificity of OmpC-binding mlgA<sub>4250</sub> and mlgA<sub>4219</sub>

and mlgA<sub>4584</sub> by recombinant purified OmpC ELISA (Extended Data Fig. 4k). Binding affinities were estimated by surface plasmon resonance (mlgA<sub>4219</sub>  $K_D = 2.50 \times 10^{-7}$  and mlgA<sub>4250</sub>  $K_D = 1.28 \times 10^{-7}$ ; Extended Data Fig. 4l). We concluded that intestinal mucosal exposure with a single transitory microbe induces antigen-specific dimeric SIgA targeting a wide range of membrane-associated antigens.

## In vivo reconstitution of secretory mlgA

To provide a scalable model to test the function of different individual monoclonal IgAs in vivo, we exploited the fact that mice secrete peripheral blood-borne dimeric IgA via bile into the intestinal lumen<sup>22,23</sup>. Negative control mlgA<sub>B8-030</sub> injected intravenously (i.v.) into JM83 mono-colonized antibody-deficient  $J_H^{-/-}$  mice resulted in transitory blood mlgA levels and faecal monoclonal SIgA (mSIgA) becoming detectable after 6 h, peaking after 9 h (Fig. 2a, b) at concentrations approximating those of colonized C57BL/6 mice<sup>24</sup>. Monomeric IgA translocation was inefficient and there were minimal levels of luminal SIgA in animals with ligated bile ducts (Extended Data Fig. 5a–c). Generally, dimeric mlgAs were efficiently secreted and coated faecal bacteria (Fig. 2c and Extended Data Fig. 5d), albeit without significant changes in colonic luminal bacterial density (Extended Data Fig. 5e).

## mlgAs show distinct functional effects

To address the functional effects of IgA in the intestine, we first reconstituted surface-binding OmpC mSIgA<sub>4250</sub> and detected downregulation



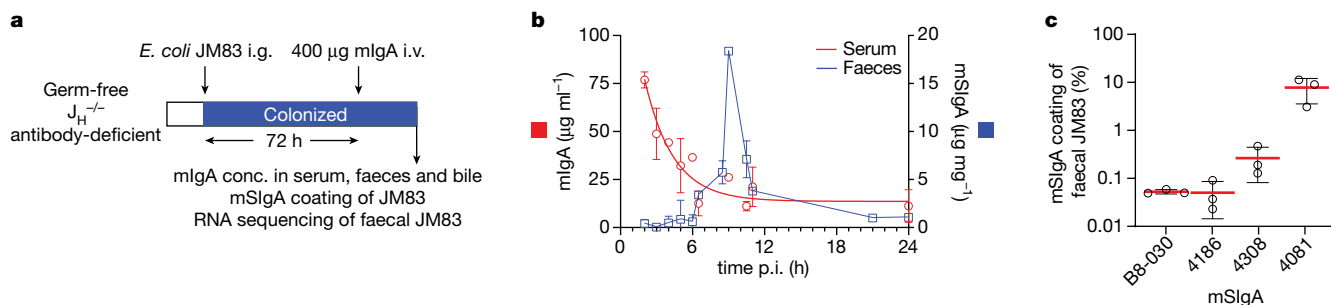


**Fig. 2 | In vivo mIgA reconstitution of antibody-deficient  $J_H^{-/-}$  mice provides a scalable model to study mSgA function.** **a**, Protocol for in vivo mIgA reconstitution in monocolonized antibody-deficient  $J_H^{-/-}$  mice. i.g., intragastric. **b**, Time course of mIgA concentration post-injection (p.i.) of antibody after i.v. mIgA<sub>B8-030</sub> reconstitution showing decay in serum (left y-axis, red) and faecal

shedding of mSgA (right y-axis, blue) ( $\bar{x} \pm s.d.$ ,  $n = 1$  to 7 mice per time point). **c**, Flow cytometric analysis of faecal mSgA-coated bacteria at 10.5 h p.i. for HA107-binding mSgA<sub>4308</sub> and mSgA<sub>4081</sub>, polyreactive mSgA<sub>4186</sub> and negative control mSgA<sub>B8-030</sub> ( $\bar{x} \pm s.d.$ ,  $n = 3$  mice for each condition). Data are from one experiment (**c**) or pooled from six independent experiments (**b**).

of *E. coli* JM83 *ompC* compared to the negative control mSgA<sub>B8-030</sub> (Extended Data Fig. 6a; qPCR verification, unpaired Student's *t*-test,  $P = 0.023$ ; Supplementary Table 5). mIgA<sub>4250</sub> reconstitution also resulted in differential expression of 9.6% of bacterial genes ( $n = 469$ ,  $P < 0.05$ ) compared with the negative control. Gene Ontology (GO) term enrichment analysis showed downregulation of genes involved in transmembrane transport of ions, carbohydrates and metabolic pathways (Fig. 3a and Supplementary Tables 6 and 7; qPCR verification *fruK*,  $P = 0.0077$ , unpaired Student's *t*-test; *ompF*,  $P = 0.0012$ ; *glpA*,  $P = 0.0322$ ; *gnd*,  $P = 0.0018$ ; Supplementary Table 5). In contrast, stress-induced genes were upregulated, including genes induced by osmotic shock or iron uptake and storage, suggesting that OmpC binding results in dysregulation of osmotic pressure (Fig. 3a and Supplementary Tables 6 and 7). Upregulation of other porins such as OmpF or LamB was not seen<sup>25</sup> (Extended Data Fig. 6b).

As with mIgA<sub>4250</sub>, mIgA<sub>4584</sub> and mIgA<sub>4219</sub> are OmpC-specific, but did not bind most live bacteria (Figs. 1c and 2e). This allowed us to show that microbial binding context critically determines functional outcome. These mSgAs neither significantly downregulated OmpC after reconstitution, nor did they phenocopy the effects of the OmpC-binder mSgA<sub>4250</sub> on the microbial transcriptome (Extended Data Fig. 6c, d). Using a cultured  $\Delta ompF$  strain (to avoid alternative porin function) we showed that mIgA<sub>4250</sub>, but not subpopulation-binding mIgA<sub>4584</sub>, reduced the capacity of <sup>14</sup>C-labelled glucose uptake (Fig. 3b), indicating that mIgA<sub>4250</sub> effectively blocks the OmpC pore. The effect of mIgA<sub>4250</sub> coating was abrogated in the double-deletion  $\Delta ompC \Delta ompF$  strain (BL21ΔCF) and could be restored upon ectopic *ompC* expression (Extended Data Fig. 6e, f). We conclude that the antigenic context in different bacterial subpopulations has a major effect on the function of the antibody on the target microbe.

OmpC is not only an outer membrane pore, but also provides T4 bacteriophage access<sup>26</sup>. We found that mIgA<sub>4250</sub>, and to a lesser degree mIgA<sub>4219</sub>, protected from T4 bacteriophage infection, compared with the negative control mIgA<sub>B8-030</sub>, the bacterial surface-binding mIgA<sub>4081</sub>, the OmpC subpopulation binder mIgA<sub>4584</sub> or the LPS binder mIgA<sub>4053</sub> (Fig. 3c). We confirmed lack of protection in a  $\Delta ompC$  strain (BL21ΔC) and restored mIgA<sub>4250</sub>-dependent protection upon ectopic OmpC expression (Extended Data Fig. 6e, g). This provided a further example of the context and specificity of mIgA binding shaping the functional outcome on the target bacterium.

To test whether our findings could be simply recapitulated by the ability of IgA to coat the bacterial surface of all subpopulations regardless of the cognate antigen, we reconstituted mice with mSgA<sub>4081</sub>, which efficiently binds nonreplicating, replicating or dying subpopulations (Fig. 1c). In vivo coating by mSgA<sub>4081</sub> did not impact the same genes as mSgA<sub>4250</sub> (Fig. 3d), instead it caused downregulation of genes enriched in cellular export, whereas upregulated gene sets included those

characteristically induced as a result of oxidative stress (Supplementary Table 8). We concluded that the specific functional effects of anti-OmpC mSgA<sub>4250</sub> are independent of the ability to coat the bacterial surface.

Given that the fine specificity of mSgA binding to bacterial OmpC produces distinctive functional effects, we next sought to confirm that different antibody-specific effects could be recapitulated using a different antibody with another defined specificity. GO term enrichment after reconstitution with fimbrial-binding mSgA<sub>4308</sub> showed downregulation of cell adhesion, cell projection and pilus organization mostly due to downregulation of genes in the *fim* operon at 10.5 h (Extended Data Fig. 6h, i and Supplementary Tables 9 and 10). After clearance of the reconstituted antibody, expression levels had recovered by 24 h (Extended Data Fig. 6j, k).

As secretory IgA against *Salmonella* leads to aggregation and enchainment<sup>2</sup>, we also addressed whether mIgA<sub>4308</sub> could cause aggregation of its *E. coli* target. Using a *fim*-locked-on strain of *E. coli* AAEC189[pSH2] to avoid phase variation of fimbrial expression, we found that mIgA<sub>4308</sub>, in contrast to OmpC-binder mIgA<sub>4250</sub>, did lead to significantly increased aggregation (Extended Data Fig. 7a–c), suggesting that IgA binding of protruding extracellular structures such as LPS O-antigen or fimbriae favours aggregation.

These results show that different IgA antigen specificities induced by microbial colonization generate distinct functional effects on target intestinal microbes in mutualistic in vivo and in vitro models. These functional effects are nongeneric in the sense that they depend on target antigen specificity and are not phenocopied purely by surface-binding effects.

## Functional impact of polyreactive mIgA

Polyreactivity has been generally inferred from the capacity for antibodies to bind to structurally diverse epitopes (double-stranded DNA, insulin and LPS) under nonblocking ELISA conditions<sup>27</sup> and is enriched in intestinal IgA<sup>1</sup>. This does not exclude antigen specificity nor infers cross-reactivity between different bacterial taxa or sub-strains<sup>28,29</sup>. We tested polyreactivity expressed as monoclonal human IgG1 for comparability with published data<sup>1,3,30</sup> by a standard polyreactivity ELISA (Extended Data Fig. 8a). We detected some weak-to-moderate polyreactive antibodies with preferential clonal expansion, mainly after mucosal bacterial priming (Extended Data Fig. 8b–e). There was no significant increase in polyreactivity in bacteria-reactive antibodies compared with monoclonal antibodies that did not specifically bind in flow cytometry or ELISA assays (Extended Data Fig. 8f), so we did not find significantly increased polyreactivity in those antibodies specifically targeting the inducing intestinal microbe.

Two polyreactive dimeric mIgAs that coated faecal microbes (mIgA<sub>4186</sub> and mIgA<sub>4250</sub>; Extended Data Fig. 8g, h) were also tested in

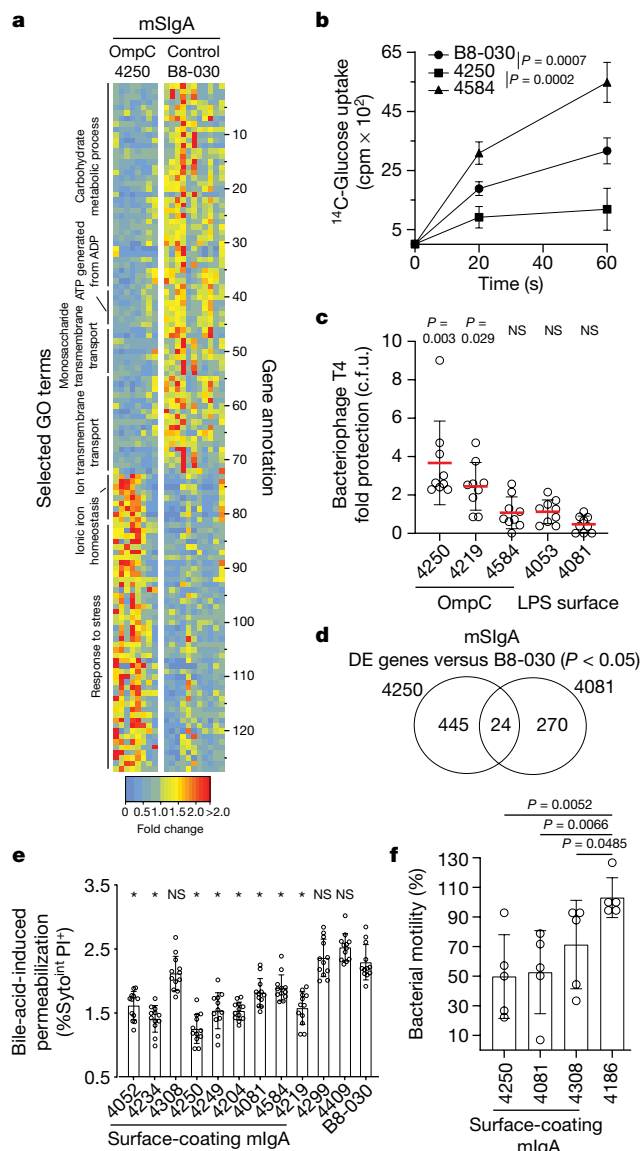


**Fig. 3 | Surface-binding mSIgA exerts antigen-dependent individual and generic functional alterations in intestinal bacteria.** **a**, Differential gene expression of enriched selected GO term gene members in faecal JM83 bacteria following reconstitution with OmpC-binding mSIgA<sub>4250</sub> as compared with negative control mSIgA<sub>B8-030</sub>. Numbers (right y axis) identify gene annotations in Supplementary Table 7. **b**, [ $^{14}\text{C}$ ] Glucose uptake in  $\Delta\text{ompF}$  bacteria coated with indicated mIgAs, ( $\bar{x} \pm \text{s.d.}$ , mSIgA<sub>B8-030</sub>  $n = 6$ , mSIgA<sub>4250</sub>  $n = 5$ , mSIgA<sub>4584</sub>  $n = 3$ ), cpm, counts per minute. **c**, Protection from bacteriophage T4 infection of mIgA-coated JM83 bacteria according to the category of the mIgA target ( $\bar{x} \pm \text{s.d.}$ ,  $n = 9$  for each condition). **d**, Venn diagram of differentially expressed (DE) genes at 10.5 h after mSIgA<sub>4250</sub> and mSIgA<sub>4081</sub> reconstitution, both compared to mSIgA<sub>B8-030</sub>. **e**, Flow cytometric analysis of faecal JM83 bacteria after exposure to bile acids. Percentages (y axis) of dying bacteria are shown (gating in Extended Data Fig. 9a) after pre-incubation with mIgA ( $\bar{x} \pm \text{s.d.}$ ,  $n = 12$  for each condition). Source data show exact  $P$  values. **f**, JM83 bacterial plate motility assay after pre-incubation with indicated mIgA ( $\bar{x} \pm \text{s.d.}$ ,  $n = 5$  for each condition). Statistics show two-sided unpaired Student's  $t$ -test (**b**, **c**, **e**, **f**),  $*P < 0.05$ ; NS, not significant. Data are pooled from two (**b**, **c**, **e**, **f**) or five (**a**, **d**) independent experiments.

the reconstitution model. In line with previous data on polyreactive IgA<sup>1</sup>, these weakly bound single glycans on a microbial/eukaryotic glycan array<sup>31</sup> (Extended Data Fig. 8i). In vivo reconstitution of polyreactive mSIgA<sub>4186</sub> compared with the control mSIgA<sub>B8-030</sub> decreased the expression of gene sets for phospholipid biosynthesis and increased the

expression of gene sets for ethanolamine metabolism and carbohydrate transport (Extended Data Fig. 8j and Supplementary Table 11). A different gene set alteration was found after polyreactive mIgA<sub>4250</sub> reconstitution (measured on *E. coli* JW2203  $\Delta\text{ompC}$  to eliminate possible effects of direct OmpC binding); only one common gene set (but containing no shared genes) was found between mSIgA<sub>4186</sub> and mSIgA<sub>4250</sub> upregulated or downregulated genes (Extended Data Fig. 8k and Supplementary Tables 11 and 12). Hence, although polyreactive mSIgAs can show individual functional effects in vivo, polyreactivity per se did not produce a consistent effect on the bacterial transcriptome in our model.

## Generic effects of surface-binding mIgAs

Given that surface-binding IgA is so widespread in the intestine, we next asked whether we could define generic functions according to surface-coating properties. We found that all surface-coating mIgAs, except for fimbrial binder mIgA<sub>4308</sub>, were able to reduce bile acid bacterial permeabilization, suggesting that surface coating, but not binding to protruding extracellular structures, can protect from bile acid-induced membrane damage (Fig. 3e and Extended Data Fig. 9a). We also observed that surface-coating mSIgA<sub>4081</sub>, mSIgA<sub>4308</sub> and mSIgA<sub>4250</sub> all downregulated genes involved in bacterial motility (Extended Data Fig. 9b and Supplementary Tables 6, 8 and 10) and reduced motility in vitro in a plate motility assay<sup>7</sup> (Fig. 3f). Therefore, individual surface-coating IgAs, independently of their antigen-dependent specific effect, exert generic functional effects on the bacteria.

In summary, clonal selection into the plasma cell IgA repertoire induced by a single microbe provides a series of SIgA-mediated parallel mechanisms, including metabolic modulation, protection from bile acids or bacteriophage, and motility alterations; these allow the immune system to exert controls in the intestinal lumen that fine-tune host–microbial mutualism. Parallelism occurs in two ways: first, the response to a single microbe has different components on distinct targets with a series of different functional results; and second, one mSIgA can have more than one functional result. Although function cannot be reliably predicted from antigen binding—as is known for responses against infectious organisms—the very parallelism of the SIgA response, here generated even by a transitory colonization by a single taxon, is probably important for constraining intestinal microbes for mutualistic behaviour within the host intestine. In these studies, we measured a series of functional SIgA responses on a single microbe that was also used as the inducing agent. In diverse microbiotas, SIgAs will probably also have direct effects of cross-reactivity between species and indirect functional effects from alterations in inter-species carbon source and electron acceptor exchange.

## Online content

Any methods, additional references, Nature Research reporting summaries, source data, extended data, supplementary information, acknowledgements, peer review information; details of author contributions and competing interests; and statements of data and code availability are available at <https://doi.org/10.1038/s41586-021-03973-7>.

- Bunker, J. J. et al. Natural polyreactive IgA antibodies coat the intestinal microbiota. *Science* **358**, eaan6619 (2017).
- Moor, K. et al. High-avidity IgA protects the intestine by enchainning growing bacteria. *Nature* **544**, 498–502 (2017).
- Benckert, J. et al. The majority of intestinal IgA<sup>+</sup> and IgG<sup>+</sup> plasmablasts in the human gut are antigen-specific. *J. Clin. Invest.* **121**, 1946–1955 (2011).
- Di Niro, R. et al. *Salmonella* infection drives promiscuous B cell activation followed by extrafollicular affinity maturation. *Immunity* **43**, 120–131 (2015).
- Sterlin, D. et al. Human IgA binds a diverse array of commensal bacteria. *J. Exp. Med.* **217**, e20181635 (2020).
- Okai, S. et al. High-affinity monoclonal IgA regulates gut microbiota and prevents colitis in mice. *Nat. Microbiol.* **1**, 16103 (2016).



7. Cullender, T. C. et al. Innate and adaptive immunity interact to quench microbiome flagellar motility in the gut. *Cell Host Microbe* **14**, 571–581 (2013).
8. Rollenske, T. et al. Cross-specificity of protective human antibodies against *Klebsiellapneumoniae* LPS O-antigen. *Nat. Immunol.* **19**, 617–624 (2018).
9. Yang, C., Chen-liaw, A., Moran, T. M., Cerutti, A. & Faith, J.J. Immunoglobulin A antibody composition is sculpted to bind the self gut microbiome. Preprint at *bioRxiv* <https://doi.org/10.1101/2020.11.30.405332> (2020).
10. Macpherson, A. J., Yilmaz, B., Limenitakis, J. P. & Ganai-Vonarburg, S. C. IgA function in relation to the intestinal microbiota. *Annu. Rev. Immunol.* **36**, 359–381 (2018).
11. Nowosad, C. R. et al. Tunable dynamics of B cell selection in gut germinal centres. *Nature* **588**, 321–326 (2020).
12. Peterson, D. A., McNulty, N. P., Guruge, J. L. & Gordon, J. I. IgA response to symbiotic bacteria as a mediator of gut homeostasis. *Cell Host Microbe* **2**, 328–339 (2007).
13. Peterson, D. A. et al. Characterizing the interactions between a naturally primed immunoglobulin A and its conserved *Bacteroides thetaiotaomicron* species-specific epitope in gnotobiotic mice. *J. Biol. Chem.* **290**, 12630–12649 (2015).
14. Lycke, N., Eriksen, L. & Holmgren, J. Protection against cholera toxin after oral immunization is thymus-dependent and associated with intestinal production of neutralizing IgA antitoxin. *Scand. J. Immunol.* **25**, 413–419 (1987).
15. Pabst, O. & Slack, E. IgA and the intestinal microbiota: the importance of being specific. *Mucosal Immunol.* **13**, 12–21 (2020).
16. Nakajima, A. et al. IgA regulates the composition and metabolic function of gut microbiota by promoting symbiosis between bacteria. *J. Exp. Med.* **215**, 2019–2034 (2018).
17. Joglekar, P. et al. Intestinal IgA regulates expression of a fructan polysaccharide utilization locus in colonizing gut commensal *Bacteroides thetaiotaomicron*. *Mbio* **10**, e02324–19 (2019).
18. Hapfelmeier, S. et al. Reversible microbial colonization of germ-free mice reveals the dynamics of IgA immune responses. *Science* **328**, 1705–1709 (2010).
19. Lindner, C. et al. Diversification of memory B cells drives the continuous adaptation of secretory antibodies to gut microbiota. *Nat. Immunol.* **16**, 880–888 (2015).
20. Maurice, C. F., Haider, H. J. & Turnbaugh, P. J. Xenobiotics shape the physiology and gene expression of the active human gut microbiome. *Cell* **152**, 39–50 (2013).
21. Li, H. et al. Mucosal or systemic microbiota exposures shape the B cell repertoire. *Nature* **584**, 274–278 (2020).
22. Hendrickson, B. A. et al. Altered hepatic transport of immunoglobulin A in mice lacking the J chain. *J. Exp. Med.* **182**, 1905–1911 (1995).
23. Johansen, F. et al. Absence of epithelial immunoglobulin A transport, with increased mucosal leakiness, in polymeric immunoglobulin receptor/secretory component-deficient mice. *J. Exp. Med.* **190**, 915–922 (1999).
24. Fransen, F. et al. BALB/c and C57BL/6 mice differ in polyreactive IgA abundance, which impacts the generation of antigen-specific IgA and microbiota diversity. *Immunity* **43**, 527–540 (2015).
25. Liu, X. & Ferenci, T. Regulation of porin-mediated outer membrane permeability by nutrient limitation in *Escherichia coli*. *J. Bacteriol.* **180**, 3917–3922 (1998).
26. Yu, F. & Mizushima, S. Roles of lipopolysaccharide and outer membrane protein OmpC of *Escherichia coli* K-12 in the receptor function for bacteriophage T4. *J. Bacteriol.* **151**, 718–722 (1982).
27. Wardemann, H. et al. Predominant autoantibody production by early human B cell precursors. *Science* **301**, 1374–1377 (2003).
28. Mouquet, H. & Nussenzweig, M. C. Polyreactive antibodies in adaptive immune responses to viruses. *Cell. Mol. Life Sci.* **69**, 1435–1445 (2011).
29. Guthmiller, J. J. et al. Polyreactive broadly neutralizing B cells are selected to provide defense against pandemic threat influenza viruses. *Immunity* **53**, 1230–1244 (2020).
30. Kabbert, J. et al. High microbiota reactivity of adult human intestinal IgA requires somatic mutations. *J. Exp. Med.* **217**, e20200275 (2020).
31. Wold, A. E. et al. Secretory immunoglobulin A carries oligosaccharide receptors for *Escherichia coli* type 1 fimbrial lectin. *Infect. Immun.* **58**, 3073–3077 (1990).

**Publisher's note** Springer Nature remains neutral with regard to jurisdictional claims in published maps and institutional affiliations.

© The Author(s), under exclusive licence to Springer Nature Limited 2021

## Methods

### Bacterial strains and culture

The following *E. coli* strains were used in this work: HA107 (ref. <sup>18</sup>) and its parental strain JM83, smooth strain BW24599 (ref. <sup>32</sup>), *fim*-locked strain AAEC189 containing plasmid pSH2 (ref. <sup>33</sup>), single defined deletion strains from the Keio collection and the parental BW25113 wild type<sup>34</sup> and outer membrane protein deletion strains BL21ΔC and BL21ΔCF<sup>35</sup> containing plasmid pGOMP<sup>36</sup>. Bacteria were grown at 37 °C (200 r.p.m.) in lysogeny broth (LB) (containing 100 μg ml<sup>-1</sup> meso-DAP and 400 μg ml<sup>-1</sup> D-alanine as required for HA107 auxotrophy). Gavage solutions were centrifuged for 10 min at 4,000g and washed twice with sterile PBS. The required dose was resuspended in 500 μl of sterile PBS and administered to germ-free mice by aseptic oral gavage.

### Bacterial fractions

Bacterial membranes, whole lysates and intracellular fractions were obtained as previously described<sup>21</sup>. Purified *E. coli* ribosomes (strain B) were obtained from New England Biolabs. Purified OmpC and LPS were obtained as previously described<sup>37,38</sup>.

Outer membrane vesicles<sup>39</sup> were prepared from 1,000 ml overnight culture of *E. coli* HA107 by centrifugation at 4,000g for 15 min at 4 °C, then passing the supernatant through a 0.45-μm filter (Merck). The filtrate was centrifuged (100,000g, 2 h, 4 °C) and after washing once in ice-cold PBS (pH 7.4) the preparation was suspended in PBS and stored at -20 °C. The presence of intact outer membrane vesicles and large extracellular structures was confirmed by transmission electron microscopy by absorption on glow-discharged and carbon-coated 400-mesh copper grids (Plano) for 1 min, before washing three times in distilled water and staining with 2% uranyl acetate solution for 45 s (Electron Microscopy Science). Results were displayed using a transmission electron microscope (80 kV, Tecnai Spirit, FEI) equipped with a digital camera (Veleta, Olympus).

Protein concentrations of all fractions were determined by BCA Protein Assay (Pierce).

### Mice and sampling

Germ-free C57BL/6 mice were bred and maintained in flexible-film isolators at the Clean Mouse Facility (University of Bern). Sex balance and age matching was ensured in all experimental groups and germ-free status was routinely monitored by culture-dependent and -independent methods. Single IgA plasma cell sorting was performed from age-matched 11–14-week-old germ-free and *E. coli* HA107-primed B6 animals and IgA reconstitution was performed in 9–14-week-old B6 J<sub>H</sub><sup>-/-</sup> animals<sup>40</sup>. All mouse experiments were performed in accordance with Swiss Federal regulations approved by the Commission for Animal Experimentation of Kanton Bern. Mucosal priming in germ-free mice was achieved by three consecutive gavages on days 0, 2 and 4 using 10<sup>10</sup> colony-forming units (c.f.u.) of *E. coli* HA107.

Polyclonal faecal SIgA fractions were obtained by flushing the isolated small intestine with 5 ml of PBS containing 0.05 M EDTA (pH 8) and 12.5 μg ml<sup>-1</sup> soybean trypsin inhibitor (Sigma) into 40 μl 100 mM phenylmethylsulfonylfluoride (Sigma). The resulting solution was centrifuged at 4,000g (10 min, 4 °C) and the supernatant was stored at -80 °C.

Faecal mSIgA was obtained by bead-beating (5 min, 30 Hz, room temperature) of fresh samples in the presence of 2 μl mg<sup>-1</sup> ice-cold PBS (pH 7.4), followed by centrifugation (12,000g, 5 min, 4 °C).

Small intestinal lamina propria lymphocytes were prepared as previously described with minor modifications<sup>21</sup>. The small intestine was placed in 1× DPBS (Gibco) on ice. Peyer's patches and fat tissue were removed and the intestine was opened longitudinally before epithelial cell separation by incubating the cut tissue with shaking for 25 min in the presence of EDTA at 37 °C. Subsequently the tissue was washed using IMDM (2% FCS) and digested using IMDM containing collagenase type IA (1 mg ml<sup>-1</sup>, Sigma) and DNase I (10 U ml<sup>-1</sup>, Roche) at 37 °C for

15–30 min. After washing, cells were frozen in aliquots of 5 × 10<sup>6</sup> cells in heat-inactivated FCS (Sigma) containing 10% dimethylsulfoxide (Sigma) using a cell-freezing container (Biocision) before storage in liquid nitrogen.

### Ig concentration and polyreactivity ELISA

Ig concentration and polyreactivity on LPS, double-stranded DNA and insulin were determined as previously described<sup>8</sup> or adapted for mouse IgA using unlabelled anti-mouse IgA coating antibody (Southern Biotech, 1:500 dilution), detection with horseradish peroxidase-conjugated anti-mouse IgA (Sigma, 1:1,000 dilution). Purified hybridoma IgA (BD Biosciences) and the polyreactive control ED38 (ref. <sup>41</sup>) or nonpolyreactive control mGO53 (ref. <sup>27</sup>) expressed with mouse IgA constant regions served as controls.

### Antigen ELISA

All antigens or bacterial fractions were coated overnight at 4 °C using a concentration of 10 μg ml<sup>-1</sup> in 50 μl or 12.5 μl PBS on 96- or 384-well high-binding ELISA plates (Costar), respectively. Plates were blocked (90 min) with 200 or 50 μl 2% BSA (w/v) in PBS pH 7.4 (Gibco). Plates were washed three times with 1× PBS pH 7.4 (Gibco) containing 0.05% Tween-20 (Sigma) and incubated with 50 or 12.5 μl serial dilutions of the indicated antibody concentrations for 1.5 h. After three further PBS washes, plates were incubated with 50 or 12.5 μl horseradish peroxidase-conjugated anti-mouse IgA and IgG detection antibody (both Sigma, 1:1,000 dilution), washed and developed using azinoethylbenzothiazoline-6-sulfonic acid (Roche). Primary and secondary antibodies were diluted in 0.5% BSA (w/v) in PBS pH 7.4 (Gibco).

### Bacterial flow cytometry and sorting

Bacteria were either cultured overnight without shaking or obtained freshly from faecal samples ex vivo and dissolved in 2 μl PBS per mg faeces. Faecal bacteria were obtained by centrifugation (15 min, 50g, 4 °C). Dilutions (25 μl) at optical density (OD)<sub>600</sub> 0.01 or a 1:100 dilution of faecal bacteria in PBS pH 7.4 containing 0.5% (w/v) BSA, respectively, were mixed with 50 μl antibody diluted at 4 μg ml<sup>-1</sup> or the indicated concentrations. After 30 min on ice, samples were centrifuged (10 min, 4,000g, 4 °C) and washed once with 200 μl PBS/BSA, before incubation on ice with 25 μl polyclonal anti-IgG Alexa647 (Jackson; 1:1,000 dilution), anti-IgA-FITC (C10-3, BD, 1:50 dilution) or BV421 (C10-1, BD, 1:20 dilution) for 30 min. After washing with PBS/BSA buffer, bacteria were resuspended in 100 μl of the same PBS/BSA buffer with appropriate combinations of 3.34 μM Syto9, 5 μM Syto61 and/or 20 μM PI. Fluorescence was acquired on a Cytoflex flow cytometer (Beckman Coulter). α-Methylmannoside was used at 100 mM to block fimbrial lectin binding before primary antibody incubation<sup>42</sup>. Antibody 4308-bound and unbound JM83 (1 × 10<sup>6</sup> c.f.u.) were sorted on a MoFlo Astrios (Beckman Coulter) into RNeasy lysis buffer (Invitrogen) and diluted 1:1 with sterile PBS before collecting the cells by centrifugation (20,000g, 10 min, 4 °C). mIgA<sub>4250</sub>-coated JM83 (1 × 10<sup>6</sup> cells) were acquired on a Imagestream X Mk II (Amnis) using a ×60 objective. The gating strategy is shown in Supplementary Fig. 1.

### Fluorescence-activated cell sorting

Frozen lamina propria cells (5 × 10<sup>6</sup>) were thawed, washed with 50 ml FACS buffer (PBS/2% FCS) and incubated with FACS buffer containing 1 μg ml<sup>-1</sup> live/dead discrimination marker 7-AAD (Invitrogen) and a combination of the following antibodies: anti-mouse B220-BV421 (RA3-6B2, BD Biosciences, 1:100 dilution); polyclonal anti-mouse IgA-FITC (Rockland, 1:100 dilution) and anti-mouse CD19-APC-H7 (1D3, BD Biosciences, 1:100 dilution). After washing with 1 ml FACS buffer, single 7-AAD<sup>-</sup>B220<sup>low</sup>IgA<sup>+</sup> cells were sorted into 384-well plates using a FACS Aria III (BD Biosciences). The gating strategy is shown in Supplementary Fig. 1.

### Single-cell Ig gene sequencing

Paired *Igh*, *Igk* and *Igl* gene amplification and sequencing from single lamina propria plasma cells was performed as previously described<sup>43</sup>.

### Recombinant human IgG1 production

For the parallel production of large numbers of human IgG1 monoclonal antibodies, V(D)J PCR amplicons from single cells were amplified as previously described<sup>44</sup> using V gene-specific forward primers and modified J gene-specific PCR reverse primers (Supplementary Table 13) and were purified using Nucleospin 96 PCR Cleanup (MACHEREY-NAGEL).

The promoter region and the *IGHG1* or *IGK* constant region of vector AbVec2.0-*IGHG1* (Addgene ID 80795) and AbVec1.1-*IGHK* (Addgene ID 80796), respectively, were amplified (1 ng DNA template, 500 nM each primer (Supplementary Table 13), 0.25 mM dNTPs (Invitrogen), 1× GC buffer and 1 U Phusion polymerase (both New England Biolabs)) from their respective vectors under the following conditions: 98 °C for 30 s, 35× (98 °C, 10 s; 60 °C, 30 s; 72 °C, 30 s), 72 °C for 10 min. Promoter and constant regions were excised and gel-purified (MACHEREY-NAGEL).

Linear Ig gene expression constructs were assembled using the promoter region, V(D)J amplicon and *IGHG1* or *IGK* constant region, by NEBuilder HiFi DNA Assembly (New England Biolabs) at an equimolar ratio of 0.03 pmol and amplified by PCR (1:50 dilution (v/v) DNA template, 500 nM CMV-IE, 500 nM SV40-ENH, 0.25 mM dNTPs (Invitrogen), 1× GC buffer and 1 U Phusion polymerase (both NEB)) under the following conditions: 98 °C for 30 s, 40× (98 °C, 10 s; 64 °C, 100 s (*IGHG1*) or 60 s (*IGK*); 72 °C for 30 s), 72 °C for 10 min. The reaction was purified using Nucleospin 96 PCR Cleanup (MACHEREY-NAGEL). DNA concentrations were determined on an M1000 microplate reader (Tecan) and primers (Supplementary Table 13) were obtained from MWG Eurofins Genomics.

To produce recombinant monoclonal IgG1, 500 ng each of the paired linear *Igγ* and *Igκ* gene expression constructs were mixed in 100 μl OptiMEM containing 3.5 μl Lipofectamine 2000 (both Invitrogen) and added to 1 ml HEK293F cells ( $0.8 \times 10^6$  cells ml<sup>-1</sup> 24 h before experimentation) in 96-well incubation plates shaking at 200 r.p.m. covered with gas-permeable sterile foil (Kisker Biotech). Serum-free Excell 293 medium (1 ml, Sigma) was added 24 h later and cells were incubated (5% CO<sub>2</sub>, 37 °C, 200 r.p.m.) for 6 days, before collecting the supernatant by centrifugation (30 min, 4,000g, 4 °C).

### Mouse dimeric IgA cloning and production

Recombinant monoclonal mouse IgA was produced by adapting a protocol for human IgG1 (ref. <sup>44</sup>). Paired *Igh* and *Igk* V(D)J amplicons were amplified by PCR using mouse V gene- and J gene-specific primers containing an AgeI and AfeI restriction site, respectively, cloned into mouse *Igα* and *Igκ* eukaryotic expression vectors and amplified in *E. coli* DH10B. Heavy and light-chain vectors and a vector encoding the joining chain (15 μg or 150 μg DNA) were PEI-mediated co-transfected in 10 ml or 100 ml HEK293F cells ( $0.8 \times 10^6$  cells ml<sup>-1</sup> 24 h before experimentation), respectively. After 24 h an equal volume of serum-free Excell 293 medium was added and cells were incubated for 6 days (5% CO<sub>2</sub>, 37 °C, 180 (20 ml culture) or 130 (200 ml culture) r.p.m.). IgA was collected by centrifuging the supernatant twice (30 min, 4 °C, 4,000g).

### Surface plasmon resonance

Monoclonal mIgA affinity was determined on a Biacore X100 (GE) using single cycle kinetics. Mouse antibody capture chips (GE) were prepared according to the manufacturer's instructions and loaded with mIgA to 180–280 relative response units. Recombinant OmpC protein was then floated over the chip surface (20 μl min<sup>-1</sup>, 80 s) at concentrations of 1.6, 8, 40, 200 and 1,000 nM and bound protein was allowed to dissociate for 60 s both in the presence of PBS containing 0.1% (w/v) *N*-decyl β-D-maltopyranoside (Sigma). Affinities were estimated using BIAevaluation software.

### mIgA reconstitution

Germ-free antibody-deficient J<sub>H</sub><sup>-/-</sup> mice<sup>40</sup> were monoclonized by oral gavage with  $5 \times 10^9$  c.f.u. JM83 (ref. <sup>45</sup>). After 72 h, each mouse received 400 μg sterile-filtered mIgA of known binding characteristics in 400 μl PBS at room temperature. To exclude potential cage effects, antibody groups were split between multiple cages. For in vivo experiments, mIgA had been concentrated by 100-kDa cutoff 15-ml spin filter columns (Merck) at 4 °C, pooled, adjusted to 15 ml with sterile ice-cold PBS pH 7.4 (Gibco), concentrated again and dialysed three times at 4 °C against 50 ml ice-cold PBS using 2-ml dialysis cassettes (Pierce).

### Bacterial RNA extraction and sequencing

Freshly obtained frozen faeces or sorted bacteria were immersed in lysis buffer (18 mM EDTA, 0.025 % SDS, 1% 2-mercaptoethanol, 95% RNA-grade formamide) dissolved and incubated at 95 °C for 7 min. After 5 min centrifugation at room temperature, the supernatant was purified by RNase-free DNase Set and RNeasy cleanup column (both QIAGEN). Integrity and quality of the RNA was confirmed on a Bioanalyzer (Agilent) and Qubit (Thermo Fisher). Before cDNA library generation, probe-based depletion of ribosomal RNA was performed on 2 μg of total RNA using a Ribominus Transcriptome Isolation kit for Yeast and Bacteria (Thermo Fisher Scientific, Invitrogen) according to the producer's protocol. Thereafter, the remaining RNA was concentrated using an RNA Clean & Concentrator-5 kit (Zymo Research) and used to make cDNA libraries using an Illumina TruSeq Stranded mRNA Library Prep kit (Illumina) in combination with IDT for Illumina, TruSeq RNA UD Indexes (Illumina). The Illumina protocol was followed exactly from the point of RNA fragmentation, omitting the initial polyA selection steps. The quantity and quality of the generated next-generation sequencing libraries were evaluated using a Qubit 4.0 fluorometer with the Qubit dsDNA HS Assay kit (Thermo Fisher Scientific) and an Advanced Analytical Fragment Analyzer System using a Fragment Analyzer NGS Fragment kit (Agilent), respectively. Pooled cDNA libraries were either single-end or paired-end sequenced using a NovaSeq 6000 reagent kit v.1.0 (100 cycles) on an Illumina NovaSeq 6000 instrument.

### Real-time qPCR with reverse transcription

Differential gene expression using real-time qPCR with reverse transcription (RT-qPCR) was assessed using the SuperScript III Platinum SYBR Green One-Step qRT-PCR kit (Invitrogen). High-quality purified bacterial RNA (2 μl with a minimum concentration of 1 ng μl<sup>-1</sup>) was mixed with 5 μl 2× SYBR Green reaction mix, 0.2 μl Superscript III RT/PlatinumTaq mix, 0.2 μl forward and reverse primer at 10 μM and 2.4 μl ultrapure water. The reaction was performed in 384-well plates (Bio-Rad) in a CFX384 Detection System (Bio-Rad) using the following protocol: 50 °C for 5 min, 95 °C for 5 min and 39× (95 °C for 15 s and 59 °C for 30 s). Differential gene expression was assessed relative to *gyrA*. Primers used are shown in Supplementary Table 14.

### Glucose uptake

Radiolabelled <sup>14</sup>Cglucose uptake was measured in ΔompF (JW0912) obtained from the Keio collection, BL21ΔCF or BL21ΔCF transformed with plasmid pGompC (induced for 2 h with 0.1 mM isopropyl-β-D-thiogalactoside) after overnight culture. Bacteria were washed once (8,000g, 3 min, 4 °C). A 220-μl portion (OD<sub>600</sub> 0.1) containing 100 μg ml<sup>-1</sup> of the indicated antibody was incubated for 30 min on ice. All the following steps were performed at room temperature. After washing once, 2.2 μl 2.5 mM [<sup>14</sup>C]glucose (0.2 mCi ml<sup>-1</sup>, Perkin Elmer) was added per tube and immediately vortexed. Serial 100-μl aliquots were removed from the reaction at the indicated times and bacteria were captured by centrifugation at 10,000g for 10 s on 0.45-μm cellulose acetate spin filter membranes (Ciro Manufacturing Corporation). Excess extracellular glucose was removed by immediately washing twice (8,000g, 10 s) with 500 μl unlabelled medium. The filter was added to

# Article

a 2-ml collection tube with 100  $\mu$ l acetic acid (Sigma) and 250  $\mu$ l tissue solubilizer (Amersham) and incubated (10 min, 58 °C). After centrifugation (10,000g, 30 s) the entire flow-through was added to 5-ml scintillation tubes containing 5 ml UltimaGOLD (PerkinElmer). Uptake of [ $^{14}$ C] glucose was measured in a TRI-CARB 2300 scintillation counter (Packard) for 5 min and expressed as average counts  $\text{min}^{-1}$ . All dilutions and washings were performed with M9 minimal medium (Sigma) supplemented with sterile 40  $\mu\text{g ml}^{-1}$  proline (Sigma), 1 mM sodium succinate (Fluka), 0.1 mM calcium chloride (Merck) and 1 mM magnesium sulfate (Sigma).

## Glycan array binding

Glycan microarray screening was performed as previously reported with minor modifications<sup>5</sup>. Monoclonal IgA or pooled sera from three specific-pathogen-free (SPF) mice were diluted in PBS containing 3% BSA (Sigma-Aldrich) to 5  $\mu\text{g ml}^{-1}$  or 50  $\mu\text{g ml}^{-1}$ , respectively and applied to the microarrays (Semiotik) for 1.5 h at 37 °C. Bound IgA was detected using 5  $\mu\text{g ml}^{-1}$  of biotinylated rat anti-mouse IgA (clone, C10-1, BD Biosciences), followed by 5  $\mu\text{g ml}^{-1}$  of Alexa Fluor 633-conjugated streptavidin (Invitrogen). Microarrays were scanned at 5- $\mu\text{m}$  resolution using a GenePix 4100A Microarray Scanner and analysed using GenePix Pro 7.3 (both from Molecular Devices). To determine specific binding of IgA to selected glycans, the ratio of relative fluorescence intensity of the samples to the control was calculated. Ratios > 2 were considered as specific binding.

## Bile-acid-induced permeabilization

Freshly isolated faecal samples were dissolved in 2  $\mu$ l PBS per mg. After centrifugation (15 min, 50g, 4 °C), a 25- $\mu$ l portion of a 1:100 dilution was mixed with 50  $\mu$ l mIgA (20  $\mu\text{g ml}^{-1}$ ) in PBS/BSA. After 30 min on ice, samples were centrifuged (10 min, 4,000g, 4 °C), and washed once with 200  $\mu$ l PBS/BSA, before incubation with 50  $\mu$ l 5 mM bile acids<sup>46</sup> (cholic acid:deoxycholic acid, 50:50; Sigma) in PBS for 30 min on ice. After washing, bacteria were resuspended in 100  $\mu$ l buffer with 3.34  $\mu\text{M}$  Syto9 and 20  $\mu\text{M}$  PI. Fluorescence was measured on a Cytotflex flow cytometer (Beckman Coulter).

## Bacteriophage infection

A static overnight culture of JM83, BL21 $\Delta$ C or BL21 $\Delta$ C transformed with plasmid pGompC (induced for 2 h with 0.1 mM isopropyl- $\beta$ -D-thiogalactoside) was washed with PBS (pH 7.4, Gibco) and 25- $\mu$ l samples ( $\text{OD}_{600}$  0.01) in PBS (pH 7.4, Gibco) were mixed with 50  $\mu$ l antibody at 20  $\mu\text{g ml}^{-1}$  diluted in PBS. After 30 min on ice, samples were centrifuged (10 min, 4,000g, 4 °C) and washed once with 200  $\mu$ l, before incubation with 50  $\mu$ l of  $8 \times 10^7$  or  $0.5 \times 10^7$  p.f.u.  $\text{ml}^{-1}$  bacteriophage T4 (Carolina) for JM83 (multiplicity of infection of 16) or BL21 $\Delta$ C (multiplicity of infection of 1), respectively for 40 min at 37 °C. After washing, the bacteria were resuspended in 100  $\mu$ l LB and plated at serial dilutions. The c.f.u. were counted and protection from lytic infection was displayed as fold protection compared to the negative control antibody B8-030.

## In vitro replication

Bacterial growth was determined in 200  $\mu$ l LB from an inoculation density of  $\text{OD}_{600}$  of 0.01 in the presence of 16  $\mu\text{g ml}^{-1}$  mIgA. Cells were incubated in sterile flat-bottom 96-well plates (Nunc) overnight, with extensive shaking every 5 min for 20 s and serial determinations of  $\text{OD}_{600}$  in a M1000 microplate reader (Tecan).

## Bacterial aggregation

An LB overnight culture containing 25  $\mu\text{g ml}^{-1}$  chloramphenicol (Sigma) of the *fim*-locked *E. coli* strain AAEC189[pSH2]<sup>33</sup> was washed three times with PBS (pH 7.4, Gibco), before 15- $\mu$ l portions ( $\text{OD}_{600}$  0.4) in PBS, pH 7.4 (Gibco) were mixed with 135  $\mu$ l antibody at 25  $\mu\text{g ml}^{-1}$  or yeast mannan (Sigma) at 0.1  $\text{mg ml}^{-1}$  diluted in PBS. After 15 min incubation at room temperature, aggregation was assessed on a DMI4000 B microscope (Leica Microsystems) with an HCX PL APO  $\times 63$  1.40-0.6 oil objective lens in bright-field mode. Images at a minimum of 18 random slide

locations per sample were acquired, aggregations were counted and displayed as aggregates per  $\text{mm}^2$ .

## Plate motility assay

Bacterial motility was performed as previously described<sup>7</sup>. Data are shown as a ratio comparing motility in the presence of the negative control antibody B8-030 and the polyclonal anti-*E. coli* flagellin rabbit IgG (Abcam) positive control.

## Bioinformatics and statistics

Ig gene features were analysed by scireptor<sup>47</sup>. Flow cytometry data were acquired using BD FACSDIVA (v.6.0) or FCAP ARRAY (v.1.0.2) and analysed using FlowJo (v.9 and v.10) software. Microscopic images were acquired using the Leica Application suite AF v.3.6 software. Quality of sequencing runs was assessed using Illumina Sequencing Analysis Viewer (v.2.4.7) and all base call files were demultiplexed and converted into FASTQ files using Illumina bcl2fastq conversion software v.2.20. GO term enrichment for biological processes was performed using the EcoCyc *E. coli* database using Fisher's exact statistical testing without multiple testing correction and a cutoff of  $P < 0.017$  (ref.<sup>48</sup>). Bacterial sequencing reads were annotated to the *E. coli* genome of strain MG1655 (U00096.2). Image plots were generated using Prism (v.8.4.3) (GraphPad) and ggplot2 and gplots packages in R (v.4.0.3). Differential gene expression analysis was performed by DEseq2 in R (v.3.6.3). Wald test and Benjamini–Hochberg correction were performed integrated in DEseq2 in R (v.3.6.3). Mann–Whitney *U*-tests, two-sided Student's *t*-tests and Fisher's exact tests were performed in Prism (v.8.4.3) (GraphPad) or R (v.4.0.3). A *P* value < 0.05 was considered significant in all experiments.

## Reporting summary

Further information on research design is available in the Nature Research Reporting Summary linked to this paper.

## Data availability

Raw sequence reads are deposited under BioProject PRJNA702008 and are associated with Fig. 3a, d and Extended Data Figs. 6a–d, h–k and 9b. Bacterial sequencing reads were annotated to the *E. coli* genome of strain MG1655 (U00096.2). GO terms and gene set members were extracted from the EcoCyc *E. coli* database at <https://ecocyc.org>. There are no restrictions on data availability. Source data are provided with this paper.

32. Stern, R. J. et al. Conversion of dTDP-4-keto-6-deoxyglucose to free dTDP-4-keto-rhamnose by the *rmlC* gene products of *Escherichia coli* and *Mycobacterium tuberculosis*. *Microbiology* **145**, 663–671 (1999).
33. Weiss, G. L. et al. Architecture and function of human uromodulin filaments in urinary tract infections. *Science* **1010**, 1005–1010 (2020).
34. Baba, T. et al. Construction of *Escherichia coli* K-12 in-frame, single-gene knockout mutants: the Keio collection. *Mol. Syst. Biol.* **2**, 2006.0008 (2006).
35. Meuskens, I., Michalik, M., Chauhan, N., Linke, D. & Leo, J. C. A new strain collection for improved expression of outer membrane proteins. *Front. Cell. Infect. Microbiol.* <https://doi.org/10.3389/fcimb.2017.00464> (2017).
36. Tran, Q.-T. et al. Structure–kinetic relationship of carbapenem antibacterials permeating through *E. coli* OmpC porin. *Proteins* **82**, 2998–3012 (2014).
37. Lukasiewicz, J. et al. Serological characterization of anti-endotoxin serum directed against the conjugate of oligosaccharide core of *Escherichia coli* type R4 with tetanus toxoid. *FEMS Immunol. Med. Microbiol.* **37**, 59–67 (2003).
38. Keegan, N., Ridley, H. & Lakey, J. H. Discovery of biphasic thermal unfolding of OmpC with implications for surface loop stability. *Biochemistry* **49**, 9715–9721 (2010).
39. Schwechheimer, C. & Kuehn, M. J. Outer-membrane vesicles from Gram-negative bacteria: biogenesis and functions. *Nat. Rev. Microbiol.* **13**, 605–619 (2015).
40. Chen, J. et al. Immunoglobulin gene rearrangement in B cell deficient mice generated by targeted deletion of the JH locus. *Int. Immunol.* **5**, 647–656 (1993).
41. Meffre, E. et al. Surrogate light chain expressing human peripheral B cells produce self-reactive antibodies. *J. Exp. Med.* **199**, 145–150 (2004).
42. Ofek, I., Mirelman, D. & Sharon, N. Adherence of *Escherichia coli* to human mucosal cells mediated by mannose receptors. *Nature* **265**, 623–625 (1977).
43. Busse, C. E., Czogiel, I., Braun, P., Arndt, P. F. & Wardemann, H. Single-cell based high-throughput sequencing of full-length immunoglobulin heavy and light chain genes. *Eur. J. Immunol.* **44**, 597–603 (2014).
44. Tiller, T., Busse, C. E. & Wardemann, H. Cloning and expression of murine Ig genes from single B cells. *J. Immunol. Methods* **350**, 183–193 (2009).

45. Li, H. et al. The outer mucus layer hosts a distinct intestinal microbial niche. *Nat. Commun.* **6**, 8292 (2015).
46. Urdaneta, V. & Casadesús, J. Interactions between bacteria and bile salts in the gastrointestinal and hepatobiliary tracts. *Front. Med.* <https://doi.org/10.3389/fmed.2017.00163> (2017).
47. Imkeller, K., Arndt, P. F., Wardemann, H. & Busse, C. E. sciReptor: analysis of single-cell level immunoglobulin repertoires. *BMC Bioinform.* **17**, 67 (2016).
48. Keseler, I. M. et al. The EcoCyc database: reflecting new knowledge about *Escherichia coli* K-12. *Nucleic Acids Res.* **45**, D543–D550 (2017).

**Acknowledgements** The Clean Mouse Facility is supported by the Genaxen Foundation, Inselspital and the University of Bern. We thank P. Nicholson, I. Keller, F. Blank, B. Haenni and staff at the flow cytometry, sequencing and microscopy core facilities of the German Cancer Research Center and University of Bern. J. Gärtner, C. Winter, D. Foster, C. Busse and R. Murugan helped with monoclonal antibody production and single-cell Ig-gene sequencing. H. Waller, D. Kalbermatter, K. Lau, R. Glockshuber, B. Yilmaz, J. Leo, C. Piselli, M. Winterhalter and J. Stanisich provided reagents and support. S. Hapfelmeier (University of Bern), provided the smooth *E. coli* strain BW24599. J. Zimmermann, F. Ronchi, H. Li, S. Ganai-Vonarburg, I. D. Young and M. Felber (University of Bern) helped with in vivo experimentation. Grant support was obtained from the Swiss National Science Foundation (310030\_179479 and Sinergia CRSII5\_177164) and European Research Council (ERC advanced grant HHMM-Neonates project no.742195) to A.J.M.; and through the Swiss National Science

Foundation (310030\_184757) and Swiss Cancer League/Swiss Cancer Research (KFS-4958-02-2020) to S.v.G. T.R. was supported by a postdoctoral long-term EMBO fellowship (ALTF 1040-2018) and funding from the Bern University Research Foundation.

**Author contributions** T.R. and A.J.M. conceived the project and designed and interpreted experiments. Experiments were carried out by T.R., with support from S.B. L.M. and S.v.G. performed glycan array analysis. J.L. performed LPS structure analysis and provided purified defined LPS samples. H.W. established and supervised the technology for monoclonal antibody selection, expression and analysis. T.R. and A.J.M. wrote the manuscript. All authors approved the manuscript.

**Competing interests** The authors declare no competing interests.

#### Additional information

**Supplementary information** The online version contains supplementary material available at <https://doi.org/10.1038/s41586-021-03973-7>.

**Correspondence and requests for materials** should be addressed to Tim Rollenske or Andrew J. Macpherson.

**Peer review information** *Nature* thanks Sidonia Fagarasan, Maria Rescigno and the other, anonymous, reviewer(s) for their contribution to the peer review of this work. Peer reviewer reports are available.

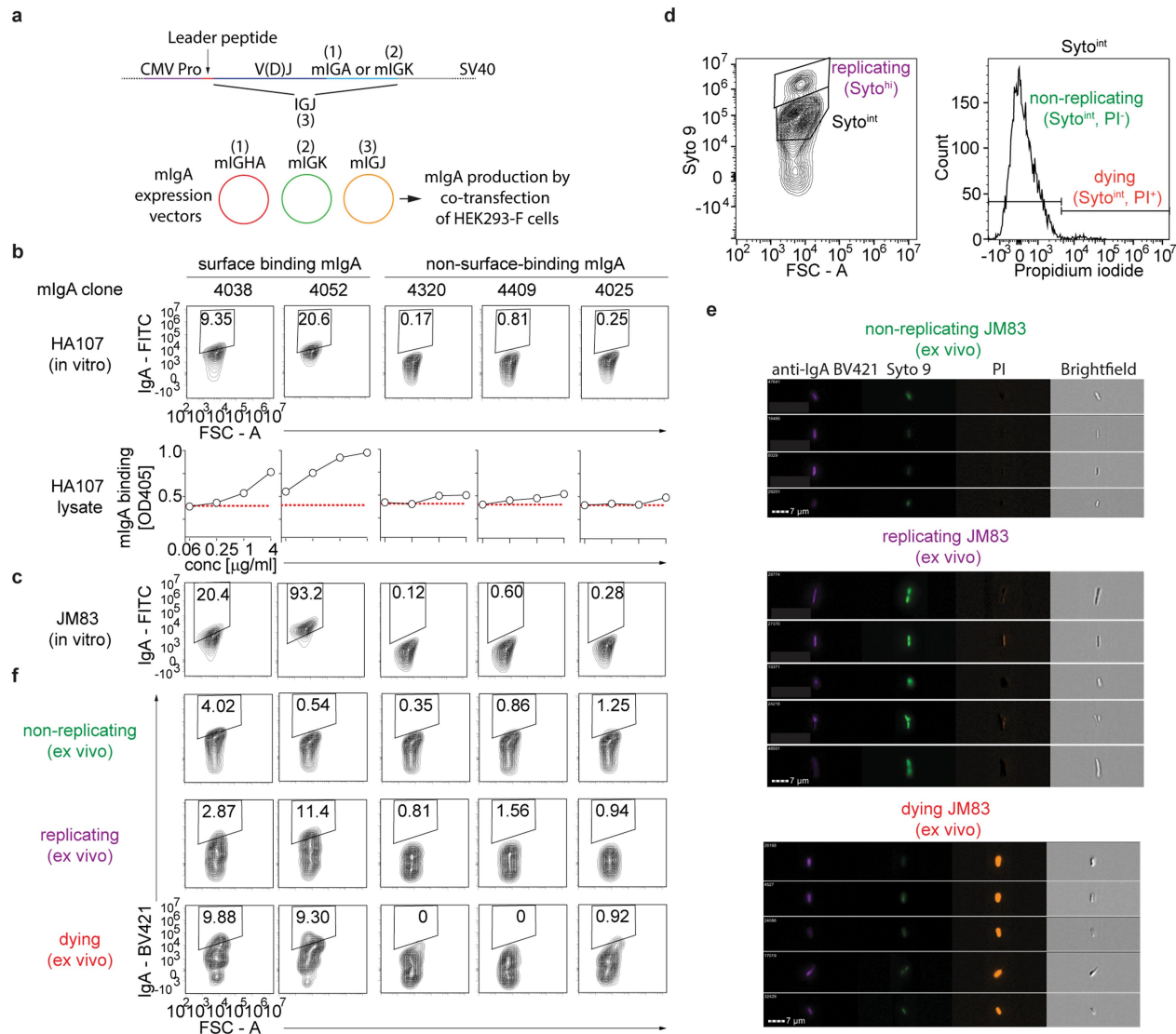
**Reprints and permissions information** is available at <http://www.nature.com/reprints>.





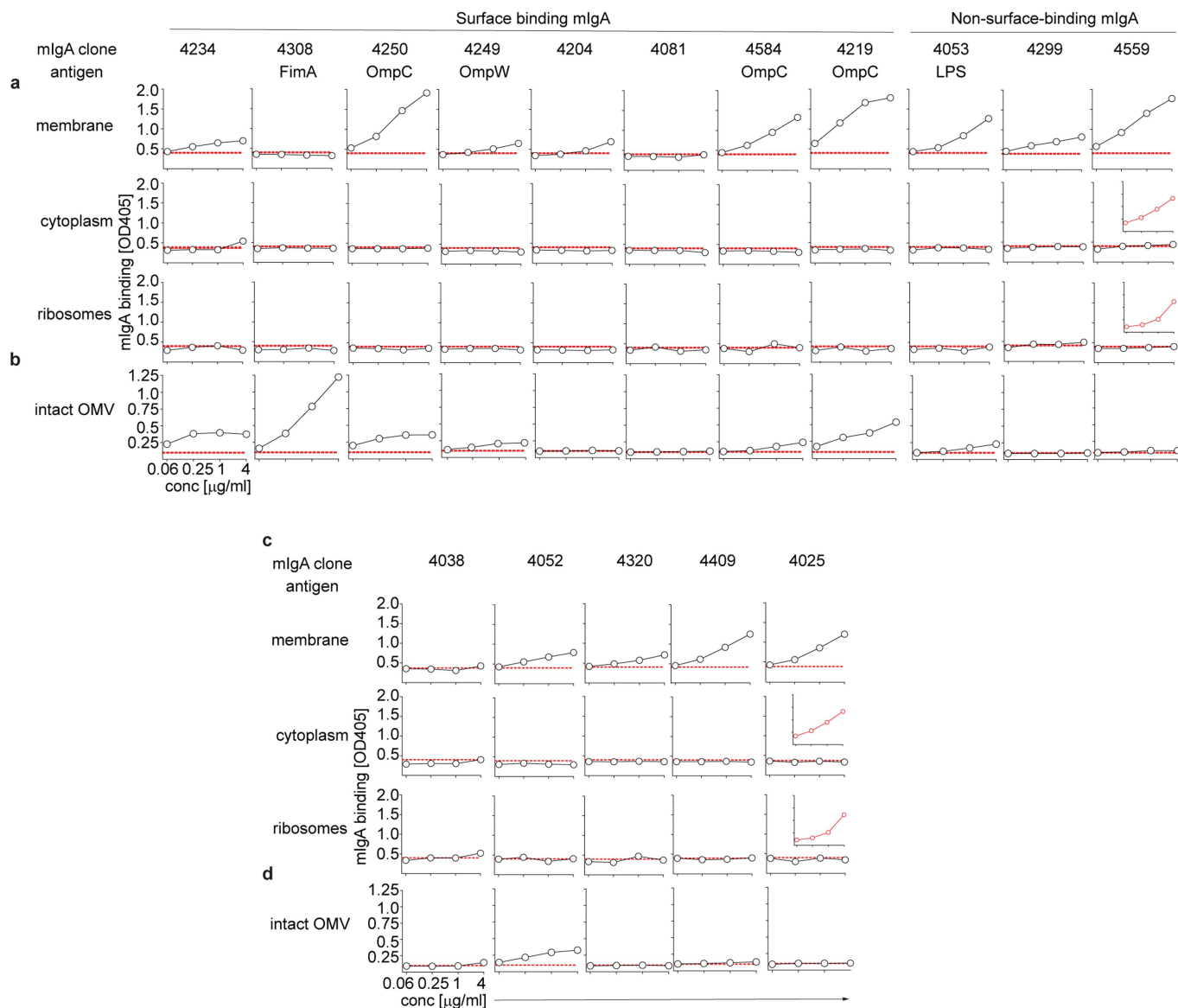
**Extended Data Fig. 1 | Ig gene and antibody-binding characteristics of monoclonal antibodies derived from intestinal plasma cells of germ-free and transitorily HA107-colonized mice.** **a**, Strategy to obtain HA107-reactive monoclonal antibodies from lamina propria plasma cells after transient intragastric (i.g.) microbial priming of germ-free wild-type (WT) mice. **b**, Flow cytometric binding analysis of luminal polyclonal SIgA derived from donor mice (each line shows a dilution series from an individual mouse,  $n = 6$ ) to intact live *E. coli* HA107, 21 days after transitory colonization. Red dashed line indicates upper limit of binding from germ-free controls. **c**, Fluorescence-activated cell sorting gate for isolation of IgA<sup>+</sup> lamina propria plasma cells for single-cell Ig sequencing, analysis and monoclonal Ig expression. **d–g**, Isotype distribution (**d**), clonal expansion (**e**) *IGHV* and *IGKV* gene combination (**f**) and number of *IGHV* somatic hypermutations (**g**) in single lamina propria plasma cell Ig gene repertoires of HA107-primed mice derived from six donor mice (**d–f**) or compared to germ-free controls obtained from six donor mice (**g**), red bar shows mean.  $n = 378$  and 379 *IGHV* sequences derived from single plasma cells from

germ-free or HA107-exposed animals, respectively (**g**). **h**, Cloning and recombinant antibody expression strategy for monoclonal human IgG1. **i**, Frequency of Igλ light-chain-expressing cells in Ig gene repertoires of HA107-primed mice compared to germ-free controls ( $n = 6$  mice), red bar shows mean. **j, k**, Flow cytometric binding analysis of live intact HA107 bacteria surface-coating monoclonal IgG1 and negative control B8-030 (**j**) showing the frequency of surface-binding IgG1 in HA107-associated antibodies and germ-free controls used at  $1 \mu\text{g ml}^{-1}$  within each animal (**k**). **l**, ELISA binding of monoclonal IgG1 derived from HA107-primed mice or germ-free controls used at  $1 \mu\text{g ml}^{-1}$  to HA107 lysate. **m**, Clonal expansions of lysate- (grey fill) and surface-binding (dark fill) monoclonal IgG1: the frequencies of B cell clusters are shown separated within the overall populations. **n**, Numbers of *IGHV* somatic hypermutations in HA107-binding ( $n = 22$ ) and nonbinding ( $n = 168$ ) antibodies and their clonal members derived from HA107-primed mice, red bars show mean values. Statistics show two-sided Mann–Whitney *U*-test (**g, n**). Data are representative of two (**b, c, j, l**) independent experiments.



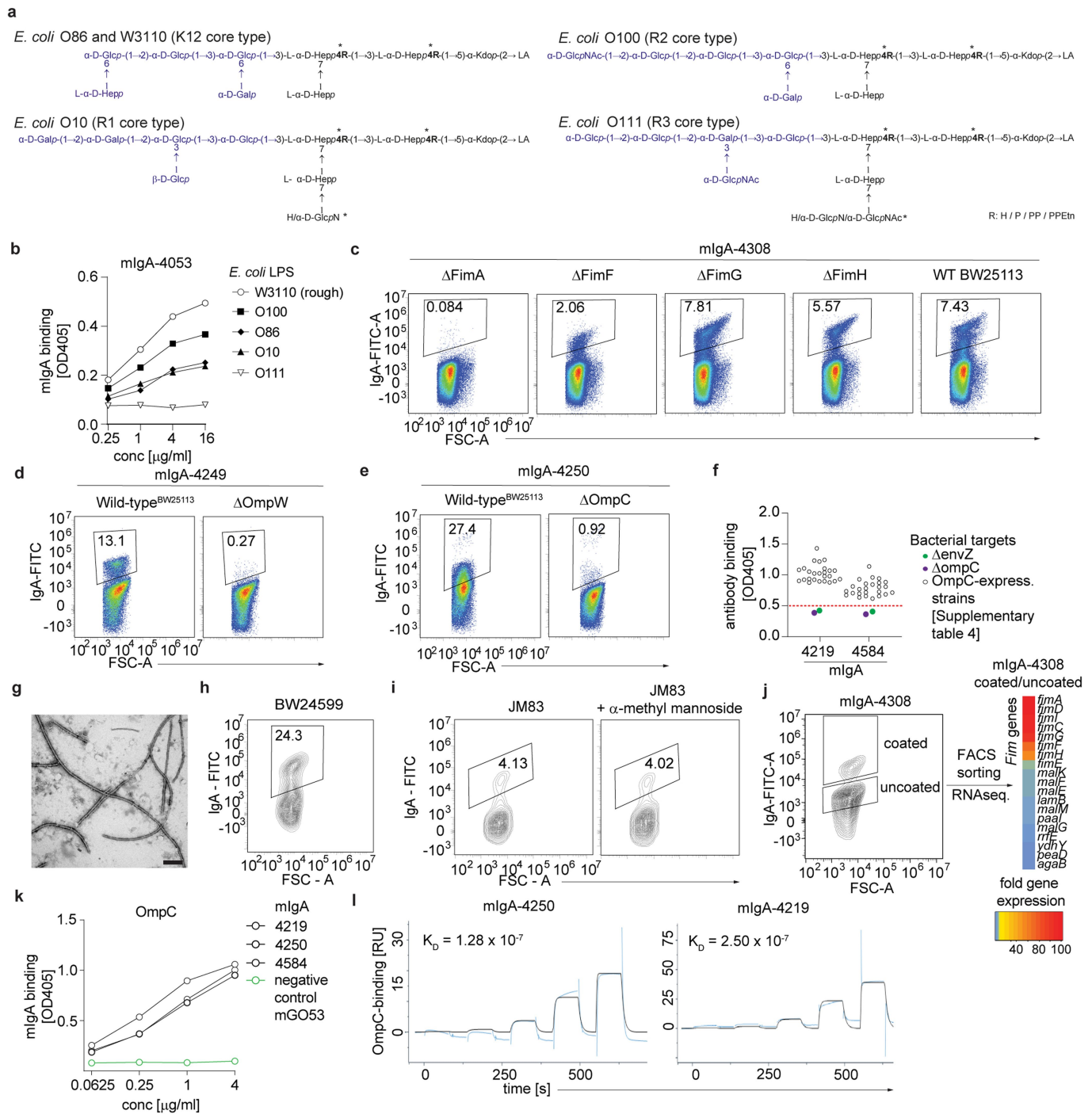
**Extended Data Fig. 2 | Antibody-binding characteristics of HA107-binding monoclonal dimeric IgA. a.** Cloning and recombinant antibody expression strategy for mouse dimeric IgA. **b, c, f.** Additional data showing further mIgAs that are not included in Fig. 1a–c due to space limitations. **b.** Individual monoclonal IgA binding to intact live HA107 bacteria by flow cytometry (top panels), or the HA107 lysate (bottom panels) by ELISA. Red dashed lines indicate cutoff for positivity. **c.** Flow cytometry analysis of mIgA binding of non-auxotrophic JM83 parental strain of HA107. **d.** Flow cytometric analysis

showing distinctive nonreplicating, replicating and dying subpopulations of JM83 isolated from fresh faecal pellets of antibody-deficient mice ex vivo. **e.** Flow cytometric microscopy of faecal JM83 nonreplicating (top), replicating (middle) and dying (bottom) subpopulations stained with mIgA<sub>4250</sub>. **f.** Binding of individual monoclonal IgAs to faecal JM83 bacterial nonreplicating, replicating or dying subpopulations gated as in Extended Data Fig. 2d. mIgA clone numbers are indicated at the top of each column (**b, c, f**). Data are of one (**e**) or representative of two (**b–d, f**) independent experiments.



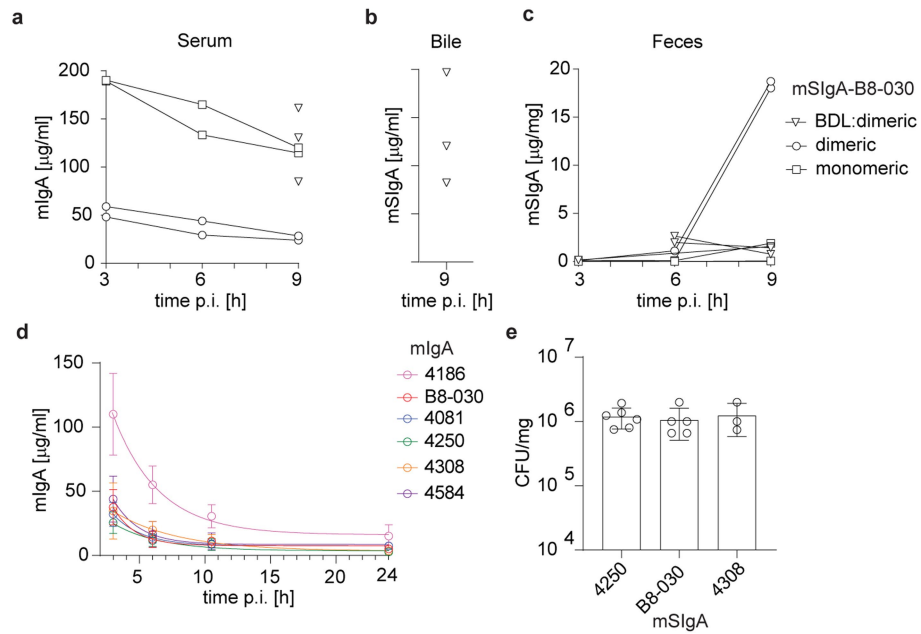
**Extended Data Fig. 3 | Intestinal dimeric mIgAs bind discrete bacterial membrane fractions. a–d**, ELISA binding of individual monoclonal dimeric IgAs ordered as in Fig. 1a–c (**a**, **b**) or Extended Data Fig. 2b, c, f (**c**, **d**) to HA107 membrane fraction (top), cytoplasmic fraction (middle) and purified ribosomes (bottom) (**a**, **c**) or intact outer membrane vesicles (**b**, **d**). mIgA clone

numbers are indicated at the top of each column. Red dashed lines indicate upper limit of binding from negative control antibody mIgA<sub>mG053</sub>. The insets within the mIgA<sub>4559</sub> (**a**, **b**) and the mIgA<sub>4025</sub> (**c**, **d**) column show control serum IgG binding from a mouse injected with  $10^8$  c.f.u. of *E. coli* HA107 14 days previously.



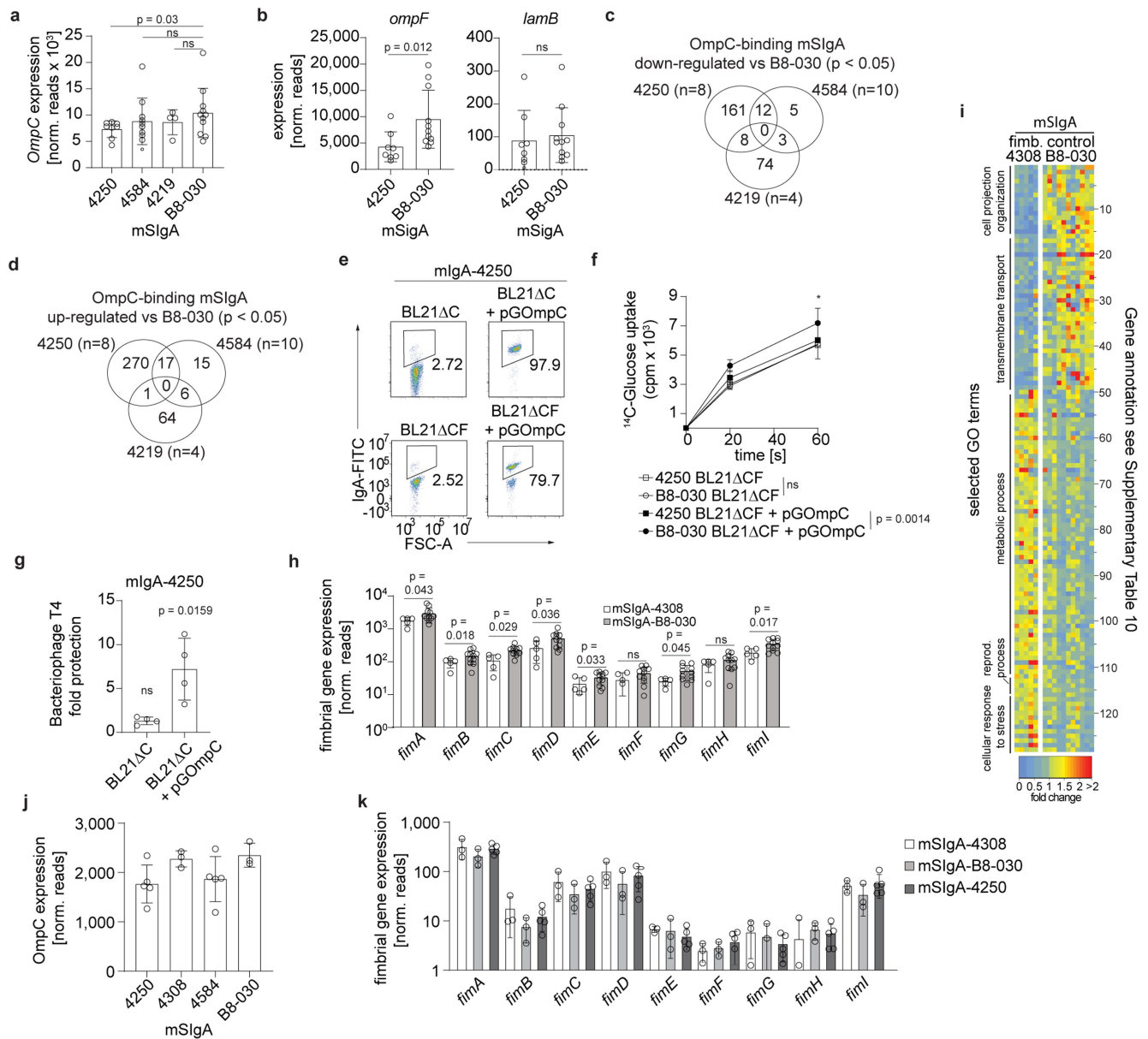
**Extended Data Fig. 4 | Intestinal dimeric mlgAs bind discrete membrane-associated antigens.** **a**, *E. coli* LPS core oligosaccharide structures (*E. coli* O86 (K12), W3110 (K12), O10 (R1), O100 (R2), and O111 (R3))<sup>37</sup>. K12, R1, R2 and R3 depict core type. R indicates nonstoichiometric substitutions; phosphate group (P); pyrophosphate group (PP); pyrophosphorylethanolamine (PPEtn). \*Indicates heterogeneity of the core OS regarding terminal sugar residues. Blue indicates outer and black indicates inner core region. LA indicates lipid A. **b**, Binding of mlgA<sub>4053</sub> to different structures of purified rough and smooth LPS shown in (a). **c**, Flow cytometric analysis of mlgA<sub>4308</sub> coating of selective fimbrial (*fim*) gene *E. coli* deletion strains<sup>34</sup> and the *E. coli* wild-type (BW25113). **d**, **e**, Flow cytometric binding analysis to *E. coli* wild-type (left) and single gene deletion strains (right) of mlgA<sub>4249</sub> (**d**) and mlgA<sub>4250</sub> (**e**). **f**, ELISA binding of indicated mlgA to lysates of *E. coli* Δ*envZ*, *E. coli* Δ*ompC*, or a series of targeted *E. coli* deletion strains, or the wild-type with normal OmpC expression (details in Supplementary Table 4). **g**, Electron micrograph of the outer membrane vesicle fraction of *E. coli*

HA107. Scale bar, 200 nm. **h**, **i**, Flow cytometric binding analysis of mlgA<sub>4308</sub> to smooth strain BW24599<sup>32</sup> (**h**) and *E. coli* JM83 pre-incubated with and without α-methyl mannoside<sup>42</sup> to block high mannose binding sites (**i**). **j**, Gene expression ratios assessed by RNA sequencing showing the 20 most upregulated genes from fractionated mlgA<sub>4308</sub> coated compared to uncoated HA107 bacteria (left), fimbrial (*fim*) operon members are highlighted (right). **k**, ELISA binding of mlgA<sub>4219</sub>, mlgA<sub>4250</sub> and mlgA<sub>4584</sub> to purified recombinant OmpC protein. Each line represents the dilution series of an individual mlgA and the negative control mlgA<sub>mGO53</sub> is shown in green. **l**, Surface plasmon resonance affinity measurements of OmpC-binding mlgA<sub>4250</sub> (left) and mlgA<sub>4219</sub> (right). Antibody affinities ( $K_D$ ) are shown in the upper left of each panel. Data were obtained from one (**g**, **j**, **l**) or are representative of two independent experiments (**b**-**f**, **h**, **i**, **k**).



**Extended Data Fig. 5 | IgA secretion and elimination in the in vivo mIgA reconstitution model.** **a,b,c** IgA concentration measurements of secretion and elimination after i.v. injection by ELISA following injection of monomeric ( $n = 2$  mice) or dimeric mIgA in unmanipulated wild-type C57BL/6 ( $n = 2$  mice) and dimeric mIgA in C57BL/6 mice ( $n = 3$ ) following bile duct ligation (BDL). Serial measurements from serum (**a**), bile (**b**) or faeces (**c**), individual data

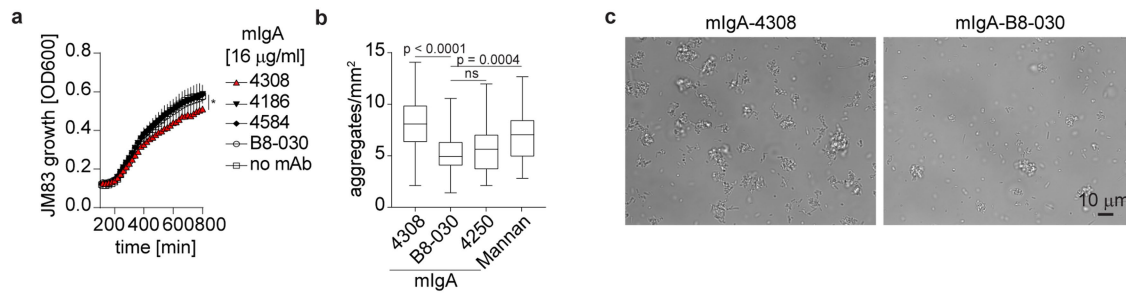
points are shown. **d**, Decay of mIgA in serum after injection of different dimeric mIgAs ( $n = 3$  for each condition;  $\bar{x} \pm \text{s.d.}$ ). **e**, c.f.u. in colonic/faecal fractions of JM83 at 10.5 h after reconstitution with the indicated mIgA species ( $\bar{x} \pm \text{s.d.}$ , mSIgA<sub>4250</sub>  $n = 6$ , mSIgA<sub>4308</sub>  $n = 3$  and mSIgA<sub>B8-030</sub>  $n = 5$  faecal samples from individual mice).



**Extended Data Fig. 6 | Functional consequences of reconstituted mSlgA in vivo and in vitro.** **a**, OmpC target gene expression from faecal JM83 bacterial RNA Sequencing analysis at 10.5 h following reconstitution with different mlgAs as shown on the x axis ( $\bar{x} \pm \text{s.d.}$ , mSlgA<sub>4250</sub>  $n = 8$ , mSlgA<sub>4584</sub>  $n = 10$ , mSlgA<sub>4219</sub>  $n = 4$  and mSlgA<sub>B8-030</sub>  $n = 10$  faecal samples from individual mice). **b**, *ompF* and *lamB* gene expression from faecal JM83 bacterial RNA sequencing at 10.5 h p.i. after mSlgA<sub>4250</sub> reconstitution ( $\bar{x} \pm \text{s.d.}$ , mSlgA<sub>4250</sub>  $n = 8$  and mSlgA<sub>B8-030</sub>  $n = 10$  faecal samples from individual mice). **c**, **d**, Venn diagrams of downregulated (**c**) or upregulated genes (**d**) after reconstitution with different OmpC-binding mSlgAs at 10.5 h p.i. **e**, Flow cytometric binding analysis of mlgA-4250 to *ompC*-deficient strain BL21ΔC (top) and BL21ΔCF (bottom) with (right) and without (left) ectopic OmpC expression<sup>35,36</sup>. Numbers adjacent to gates indicate bound bacterial frequencies. **f**, [ $^{14}\text{C}$ ]Glucose uptake in BL21ΔCF bacteria with or without pGOmpC complementation coated with indicated mlgA, ( $\bar{x} \pm \text{s.d.}$ , mSlgA<sub>B8-030</sub>  $n = 5$  with and 3 without pGOmpC, mSlgA<sub>4250</sub>  $n = 6$  with and 3 without pGOmpC). **g**, Protection from bacteriophage T4 infection of

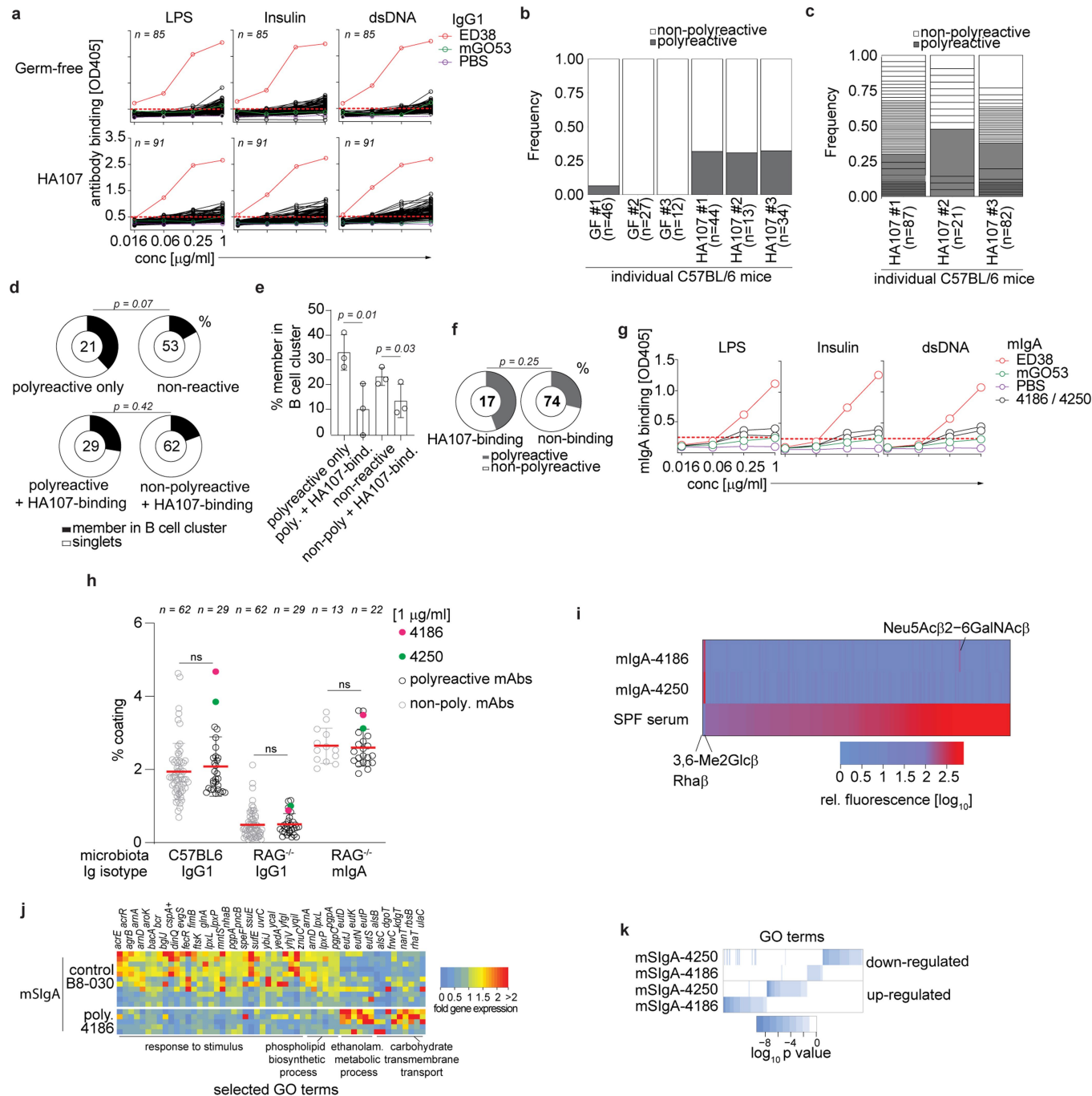
mlgA-4250-coated OmpC-deletion and complemented bacteria ( $\bar{x} \pm \text{s.d.}$ ,  $n = 4$  for each condition). **h**, Fimbrial operon members target gene expression from faecal JM83 bacterial RNASeq analysis at 10.5 h following reconstitution with different mlgAs as shown on the x axis ( $\bar{x} \pm \text{s.d.}$ , mSlgA<sub>4308</sub>  $n = 5$  and mSlgA<sub>B8-030</sub>  $n = 10$  faecal samples from individual mice). **i**, Differential gene expression of enriched GO term gene members in faecal JM83 bacteria after reconstitution with fimbriae (fimb.)-binding mSlgA<sub>4308</sub> and negative control mSlgA<sub>B8-030</sub>. Numbers (right y axis) identify gene annotations in Supplementary Table 10. **j**, **k**, mSlgA target gene expression from faecal JM83 bacterial RNA sequencing 24 h following mlgA reconstitution, at a time when mSlgA had been almost completely shed from the animal via the faeces ( $\bar{x} \pm \text{s.d.}$ , individual data points are shown). Compare 10.5 h in **a** and **h**. Statistics show two-sided Wald test (**a**, **b**, **h**) and two-sided paired (**f**) and unpaired *t*-test (**g**),  $*P < 0.05$ . Data are from one experiment (**k**) or representative from two experiments (**e**) or pooled from two (**f**, **g**, **j**), four (**a**, **b**, **h**) and five (**c**, **d**, **i**) independent experiments.





**Extended Data Fig. 7 | Bacterial aggregation of mlgA-4308. a**, OD of *E. coli* JM83 grown in the presence of mlgA ( $\bar{x} \pm \text{s.d.}$ ,  $n = 4$  for each condition,  $\text{mlgA}_{4308} P = 0.0054$ ). **b, c**, Bacterial aggregates of *fim*-locked *E. coli* strain AAEC189[pSH2]<sup>33</sup> after addition of mlgA or yeast mannan quantified (**b**) and as representative images (**c**). Box plot shows mean and 25–75th percentiles,

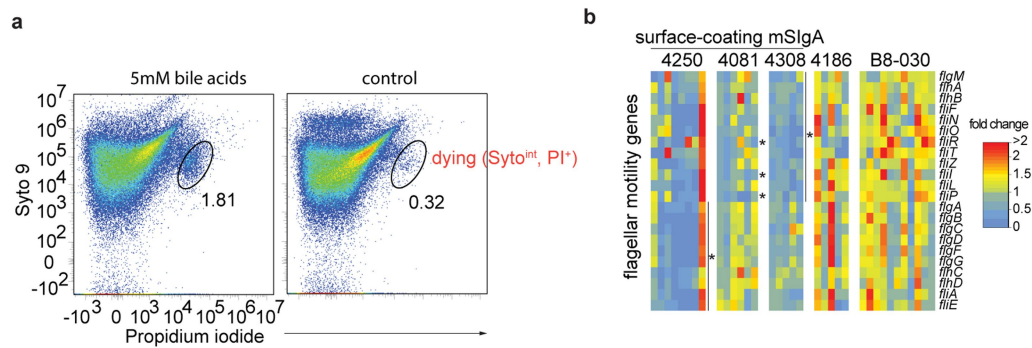
whiskers show minimum and maximum value (**b**).  $\text{mSlgA}_{4308} n = 68$ ,  $\text{mSlgA}_{\text{B8-030}} n = 70$ , Mannan  $n = 58$  and  $\text{mSlgA}_{4250} n = 68$ . Bar corresponds to 10  $\mu\text{m}$ . Statistics show two-sided paired *t*-test (**a**) and two-sided unpaired *t*-test (**b**). Data are representative from three experiments (**c**) or pooled from two (**a**) or three (**b**) independent experiments.



Extended Data Fig. 8 | See next page for caption.

**Extended Data Fig. 8 | Properties of polyreactive monoclonal antibodies derived from plasma cells of germ-free and HA107-primed mice.** **a**, ELISA binding of monoclonal IgG1 derived from plasma cells of germ-free ( $n = 85$  monoclonal antibodies, top) and HA107-primed mice ( $n = 91$  monoclonal antibodies, lower row) using standard polyreactivity measurement conditions<sup>27</sup> to LPS O111:B4 (left panels), insulin (middle) and double-stranded (ds) DNA (bottom). Red dashed lines show cutoffs according to convention: red and green lines show positive and negative control antibodies mIgG1<sub>ED38</sub> and mIgG1<sub>mGO53</sub>, respectively. **b**, **c** Polyreactive antibody frequencies among all tested antibodies ordered by donor mouse (**b**) or clonal frequencies for HA107-primed mice (**c**). **d**, **e**, Summary data of frequency of antibodies that are clonally-expanded among polyreactive (upper left) or nonreactive antibodies (upper right) or including HA107-binders (lower left and right respectively) among all expressed antibodies (**d**) and per HA107-primed donor animal (**e**). Number of antibodies per group is indicated (**d**).  $\bar{x} \pm \text{s.d.}$ ,  $n = 3$  mice for each condition (**e**). **f**, Frequency of polyreactive antibodies within HA107-binding (left) and nonbinding (right) antibodies. Number of antibodies per group is indicated. **g**, ELISA binding of mIgA<sub>4250</sub> and mIgA<sub>4186</sub> to LPS (left), insulin

(middle) and double-stranded (ds) DNA (right). Red dashed lines show cutoffs according to the highest value of the mIgA<sub>mGO53</sub> negative control, red and green lines show positive and negative control antibodies mIgA<sub>ED38</sub> and mIgA<sub>mGO53</sub>, respectively. **h**, Flow cytometric binding analysis of polyreactive (black) and nonpolyreactive (light grey) IgG1 and mIgA to faecal bacteria pooled from C57BL/6 SPF ( $n = 6$ ) or RAG<sup>-/-</sup> ( $n = 2$ ) animals ( $\bar{x} \pm \text{s.d.}$ ). Number of antibodies tested is indicated at the top of each group. Red and green symbols show polyreactive antibodies 4186 and 4250, respectively. **i**, Glycan array binding of mIgA<sub>4186</sub>, mIgA<sub>4250</sub> and pooled SPF control serum ( $n = 3$ ). **j**, Differential gene expression of enriched GO term gene members in faecal JM83 bacteria after reconstitution with polyreactive mSIgA<sub>4186</sub> and negative control mSIgA<sub>B8-030</sub>. **k**, Differential gene expression of enriched GO terms in faecal JM83 and JW2203( $\Delta ompC$ ) bacteria after reconstitution with polyreactive mSIgA<sub>4186</sub>, mSIgA<sub>4250</sub> and negative control mSIgA<sub>B8-030</sub>. Statistics show two-sided Fisher's Exact (**d**, **f**), two-sided unpaired  $t$ -test (**e**) and two-sided Mann-Whitney  $U$ -test (**h**) +  $P_{\text{adj}} < 0.1$ . Data are obtained from one (**h**, **k**), representative from two (**g**, **i**) or three (**a**) and pooled from five (**j**, **k**) independent experiments.



**Extended Data Fig. 9 | Generic functional effects of surface-coating mSlgA.**

**a**, Flow cytometric live/dead analysis to faecal *E. coli* JM83 with (left) or without (right) preincubation with bile acids. **b**, DE flagellar motility genes after indicated mSlgA reconstitution (*P* values mSlgA<sub>4308</sub>: *flgMP* = 0.038, *flhAP* = 0.036, *flhB* *P* = 0.044, *fliFP* = 0.035, *fliNP* = 0.048, *fliOP* = 0.015, *fliRP* = 0.002, *fliTP* = 0.003,

*fliZP* = 0.037, *fliIP* = 0.008, *fliLP* = 0.028, *fliPP* = 0.042; mSlgA<sub>4081</sub>: *fliRP* = 0.010, *fliIP* = 0.035, *fliPP* = 0.013; mSlgA<sub>4250</sub>: *flgAP* = 0.028, *flgBP* = 0.025, *flgCP* = 0.014, *flgDP* = 0.042, *flgFP* = 0.019, *flgGP* = 0.049, *flhCP* < 0.001, *flhDP* = 0.030, *fliA* *P* = 0.019, *fliEP* = 0.025). Data are representative from two (**a**) or five (**b**) independent experiments.

## Reporting Summary

Nature Research wishes to improve the reproducibility of the work that we publish. This form provides structure for consistency and transparency in reporting. For further information on Nature Research policies, see [Authors & Referees](#) and the [Editorial Policy Checklist](#).

### Statistics

For all statistical analyses, confirm that the following items are present in the figure legend, table legend, main text, or Methods section.

n/a Confirmed

- ☐ ☒ The exact sample size ( $n$ ) for each experimental group/condition, given as a discrete number and unit of measurement
- ☐ ☒ A statement on whether measurements were taken from distinct samples or whether the same sample was measured repeatedly
- ☐ ☒ The statistical test(s) used AND whether they are one- or two-sided  
*Only common tests should be described solely by name; describe more complex techniques in the Methods section.*
- ☒ ☐ A description of all covariates tested
- ☐ ☒ A description of any assumptions or corrections, such as tests of normality and adjustment for multiple comparisons
- ☐ ☒ A full description of the statistical parameters including central tendency (e.g. means) or other basic estimates (e.g. regression coefficient) AND variation (e.g. standard deviation) or associated estimates of uncertainty (e.g. confidence intervals)
- ☐ ☒ For null hypothesis testing, the test statistic (e.g.  $F$ ,  $t$ ,  $r$ ) with confidence intervals, effect sizes, degrees of freedom and  $P$  value noted  
*Give  $P$  values as exact values whenever suitable.*
- ☐ ☒ For Bayesian analysis, information on the choice of priors and Markov chain Monte Carlo settings
- ☐ ☒ For hierarchical and complex designs, identification of the appropriate level for tests and full reporting of outcomes
- ☒ ☐ Estimates of effect sizes (e.g. Cohen's  $d$ , Pearson's  $r$ ), indicating how they were calculated

*Our web collection on [statistics for biologists](#) contains articles on many of the points above.*

### Software and code

Policy information about [availability of computer code](#)

#### Data collection

Flow cytometry data were acquired using BD FACSDIVA (v6.0) or FCAP ARRAY (v1.0.2) software. Sequence base call files were demultiplexed and converted into FASTQ files using illumina bcl2fastq conversion software version 2.20. Microscopic images were acquired using the Leica Application suite AF v3.6.

#### Data analysis

Data analysis was carried out with FlowJo v9 and 10, Prism v8.4.3, R v3.6.3 and R v4.0.3. Ig gene features were analyzed by scireptor available at <https://github.com/b-cell-immunology/sciReptor>. Quality of the sequencing runs was assessed using illumina Sequencing Analysis Viewer (version 2.4.7). Differential gene expression analysis was performed by DESeq2 in R (v3.6.3). Gene-ontology (GO) term enrichment for biological processes was performed using the EcoCyc E. coli database.

For manuscripts utilizing custom algorithms or software that are central to the research but not yet described in published literature, software must be made available to editors/reviewers. We strongly encourage code deposition in a community repository (e.g. GitHub). See the Nature Research [guidelines for submitting code & software](#) for further information.

### Data

Policy information about [availability of data](#)

All manuscripts must include a [data availability statement](#). This statement should provide the following information, where applicable:

- Accession codes, unique identifiers, or web links for publicly available datasets
- A list of figures that have associated raw data
- A description of any restrictions on data availability

The raw files for the datasets generated during this study will be available on the SRA repository (bioproject PRJNA702008) and are associated to Figure 3a,d and Extended Data Figure 6a-d, h-k and 9b. Source data is available for Fig. 2b, 3b,e, Extended Data Fig. 5a-d, 6f and 7a,b. Bacterial sequencing reads were annotated to the E. coli genome of strain MG1655 (U00096.2). Gene-ontology (GO) terms for biological processes was performed using the EcoCyc E. coli database (<https://ecocyc.org>). There are no restrictions on data availability.

## Field-specific reporting

Please select the one below that is the best fit for your research. If you are not sure, read the appropriate sections before making your selection.

☒ Life sciences ☐ Behavioural & social sciences ☐ Ecological, evolutionary & environmental sciences

For a reference copy of the document with all sections, see [nature.com/documents/nr-reporting-summary-flat.pdf](https://nature.com/documents/nr-reporting-summary-flat.pdf)

## Life sciences study design

All studies must disclose on these points even when the disclosure is negative.

|                 |                                                                                                                                                                                                                                                                                                                                                                                                                                                                                                                                                                                                                      |
|-----------------|----------------------------------------------------------------------------------------------------------------------------------------------------------------------------------------------------------------------------------------------------------------------------------------------------------------------------------------------------------------------------------------------------------------------------------------------------------------------------------------------------------------------------------------------------------------------------------------------------------------------|
| Sample size     | The frequency of bacteria-reactive intestinal plasma cells after gavage has not been reported, therefore sample size was not predetermined. To accommodate for potential inter-donor variability we used 6 donor animals being three more than common in the field. Bacteria-reactive antibodies were identified from every donor (6/6) analyzed by flow cytometry. Bacteria-reactive antibodies were cloned from 3 animals. Since all donor animals showed these cells we considered the sample size sufficient.                                                                                                    |
| Data exclusions | No data points were excluded from the analysis.                                                                                                                                                                                                                                                                                                                                                                                                                                                                                                                                                                      |
| Replication     | Experiments were repeated at least once or twice. The only exceptions were experiments that included unique cellular material (for single cell Ig gene repertoires) because of the destruction of the sample during processing and Fig. 2c; Ext. Data. Fig. 2e, 4j,l, 5a-e and 6k. Animal experiments carried out once were to limit ethical animal use and enable resources for a series of complementary experiments. Targeting of type I fimbriae by mlgA-4308 shown in Fig. 4j was independently confirmed by other methods and was not repeated. All replication attempts throughout the paper were successful. |
| Randomization   | Mice were randomly allocated to gavage or mlgA injection treatment groups. No further group allocation was performed.                                                                                                                                                                                                                                                                                                                                                                                                                                                                                                |
| Blinding        | Blinding was performed for image analysis shown Extended Data Fig. 7b. For all other experiments blinding during data collection was not performed as all measurements were objectively quantifiable.                                                                                                                                                                                                                                                                                                                                                                                                                |

## Reporting for specific materials, systems and methods

We require information from authors about some types of materials, experimental systems and methods used in many studies. Here, indicate whether each material, system or method listed is relevant to your study. If you are not sure if a list item applies to your research, read the appropriate section before selecting a response.

### Materials & experimental systems

|                                     |                                                                 |
|-------------------------------------|-----------------------------------------------------------------|
| n/a                                 | Involved in the study                                           |
| <input type="checkbox"/>            | <input checked="" type="checkbox"/> Antibodies                  |
| <input type="checkbox"/>            | <input checked="" type="checkbox"/> Eukaryotic cell lines       |
| <input checked="" type="checkbox"/> | <input type="checkbox"/> Palaeontology                          |
| <input type="checkbox"/>            | <input checked="" type="checkbox"/> Animals and other organisms |
| <input checked="" type="checkbox"/> | <input type="checkbox"/> Human research participants            |
| <input checked="" type="checkbox"/> | <input type="checkbox"/> Clinical data                          |

### Methods

|                                     |                                                    |
|-------------------------------------|----------------------------------------------------|
| n/a                                 | Involved in the study                              |
| <input checked="" type="checkbox"/> | <input type="checkbox"/> ChIP-seq                  |
| <input type="checkbox"/>            | <input checked="" type="checkbox"/> Flow cytometry |
| <input checked="" type="checkbox"/> | <input type="checkbox"/> MRI-based neuroimaging    |

## Antibodies

### Antibodies used

Flow cytometry antibodies:  
 anti-mouse B220-BV421 (RA3-6B2, BD Biosciences) 1:100;  
 polyclonal anti-mouse IgA-FITC (Rockland) 1:100;  
 anti-mouse CD19-APC-H7 (1D3, BD Biosciences) 1:100;  
 polyclonal anti-human IgG Alexa647 (Jackson) 1:1000;  
 anti-mouse IgA FITC (C10-3, BD, 1:50);  
 anti-mouse IgA BV421 (C10-1, BD, 1:20)

ELISA antibodies:  
 anti-mouse IgA (Southern biotech) 1:500;  
 Purified mouse IgA (BD)  
 Anti-mouse IgG  $\gamma$  chain specific-peroxidase conjugated (Sigma) 1:1000;  
 Anti-mouse IgA  $\alpha$  chain specific-peroxidase conjugated (Sigma) 1:1000.

Used for human IgG1 concentration measurement described in reference 8:  
 Purified human IgG1, kappa (Sigma);



## Validation

Anti human IgG Fc detection antibody (Jackson) 1:1000;  
anti-human IgG Fc fragment specific (Jackson) 1:500.

Flow cytometry antibodies used to identify lamina propria plasma cells and to detect mouse IgA have been validated as described by the manufacturer and by serial titration of the antibody on pre-defined single cell suspensions of mouse small intestinal tissue. ELISA antibodies were validated by the manufacturer to be human or mouse-specific and were re-validated on commercially available antigen targets.

## Eukaryotic cell lines

Policy information about [cell lines](#)

Cell line source(s) HEK293F cells (R79007) were purchased from Thermo Fisher.

Authentication HEK293F cells were not authenticated

Mycoplasma contamination HEK293-F cells were not tested for mycoplasma contamination

Commonly misidentified lines  
(See [ICLAC](#) register) No commonly misidentified cell lines were used in this study.

## Animals and other organisms

Policy information about [studies involving animals](#); [ARRIVE guidelines](#) recommended for reporting animal research

Laboratory animals Mice used in this study were housed in the Clean Mouse Facility of the University of Bern. All mice were born and raised sterilely and kept in sterile flexible film isolators with 12h/12h light/dark cycle, 22-25°C and 40-42% humidity. C57BL/6 mice were used (9-14 weeks of age of mixed gender).

Wild animals The study did not involve wild animals.

Field-collected samples The study did not involve samples collected from field studies.

Ethics oversight All mouse experiments were performed in accordance with Swiss Federal and Cantonal regulations. Permission was granted by the Commission for animal experimentation of the Kanton Bern.

Note that full information on the approval of the study protocol must also be provided in the manuscript.

## Flow Cytometry

### Plots

Confirm that:

- ☒ The axis labels state the marker and fluorochrome used (e.g. CD4-FITC).
- ☒ The axis scales are clearly visible. Include numbers along axes only for bottom left plot of group (a 'group' is an analysis of identical markers).
- ☒ All plots are contour plots with outliers or pseudocolor plots.
- ☒ A numerical value for number of cells or percentage (with statistics) is provided.

### Methodology

Sample preparation Small intestinal lamina propria lymphocytes were prepared as previously described with minor modifications. The small intestine was placed in 1x DPBS (Gibco) on ice. Peyer's patches and fat tissue were removed, and the intestine opened longitudinally before epithelial cell separation by incubating the cut tissue with shaking for 25 minutes in the presence of EDTA at 37°C. Subsequently the tissue was digested using IMDM (2% FCS) containing collagenase type IA (1 mg/ml, Sigma) and DNase I (10 U/ml, Roche) at 37°C for 20-30 min. After washing, cells were frozen in aliquots of 5x10<sup>6</sup> cells in heat-inactivated FCS (Sigma) containing 10% DMSO (Sigma) using a cell freezing container (Biocision) before storage in liquid nitrogen.

Instrument BD Aria III, Beckman Coulter CytoFlex, Beckman Coulter MoFlo.

Software BD FACSDiva (v6.0) for collection and FlowJo (versions 9 and 10) for analysis.

Cell population abundance Purity of each sorted sample was over 90% as confirmed by re-acquisition on the sorter (MoFlo).

Gating strategy Lamina propria plasma cells were gated as single, 7-AAD-, B220lo, IgA+. Bacterial populations were gated on bacteria using FSC/SSC in log display and an empty flow cytometry buffer control and further on Syto+ cells. Gating borders were established using isotype controls for bacterial flow cytometry and fluorescence-minus-one controls for intestinal lamina propria plasma cells. Detailed gating strategies used are shown in Supplementary Figure 1.

☒ Tick this box to confirm that a figure exemplifying the gating strategy is provided in the Supplementary Information.